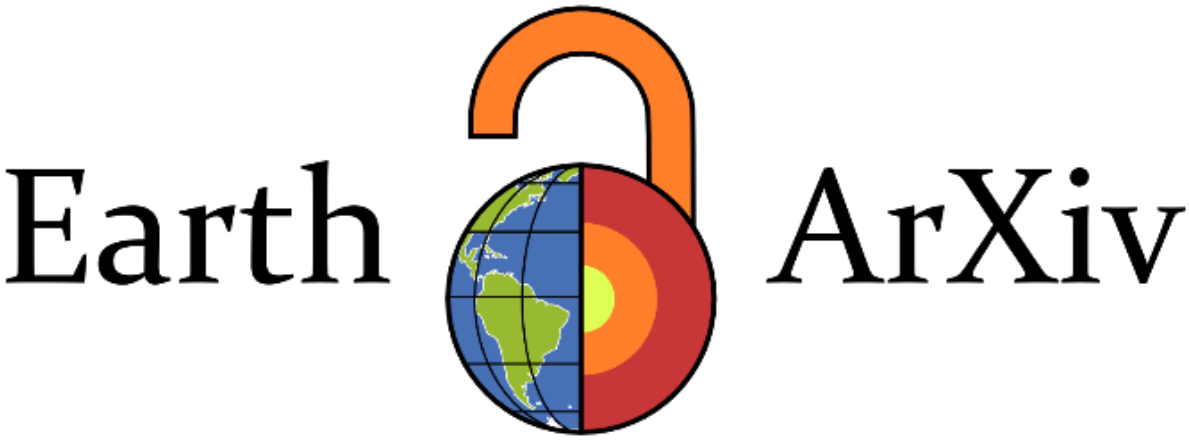


Peer review status:

This is a non-peer-reviewed preprint submitted to EarthArXiv.

Is 50.0 °C possible in West Athens?

Panagiotis Douros[1,*], Alfio Grassi[2]

[1]Adjunct Faculty, Department of Health Science, University of the People (UoPeople), United States

[2]Regional Order of Geologists of Sicily (ORGS, Reg. No. 2352), Catania, Italy

*Corresponding author: panagiotis.douros@uopeople.edu | ORCID: https://orcid.org/0009-0006-6053-257X

Co-author: etnageo@libero.it | ORCID: https://orcid.org/0009-0004-4969-2498

Abstract

We examine summer daily maximum temperature differentials across nine stations in West Athens (Thriasio Plain), where historical peaks reached $48.0°$C (July 1977, all-time European mainland record), $47.5°$C (June 2007, European June record), and $47.0°$C (July 1973). Although the World Meteorological Organization (WMO) ratified $48.8°$C in Sicily (2021), a reading currently under metrological dispute, the $48.0°$C Elefsina observation from Hellenic National Meteorological Service (HNMS) synoptic records remains the European mainland record. Across 2024–2026, the automated HNMS Microstep-MIS station at Elefsina Airport read $+0.86 \pm 0.38°$C ($p < 10^{-16}$) above the co-located Stevenson screen. Over the full set of 399 paired days, the fan-aspirated National Observatory of Athens (NOA) station in Elefsina Town stayed within $+0.15 \pm 0.49°$C of the screen. In JJA 2026, Aspropyrgos Coast NOA averaged $34.90°$C, exceeding Aspropyrgos Town by $+1.47°$C, Elefsina Classical by $+1.39°$C, and Elefsina Town by $+1.26°$C. Its JJA 2024 mean is estimated at 37.11–$37.43°$C. During katabatic Foehn peaks, the coastal strip averaged $+2.08°$C warmer than Elefsina Classical and reached a $+2.8°$C daily excess. Cross-station validation on June 26, 2007 reproduces the $47.5°$C Aspropyrgos municipal record within $0.1°$C. Superposing modern katabatic offsets onto the $48.0°$C Elefsina record of July 10, 1977 yields a shield-adjusted coastal estimate of $49.9°$C, with a 49.2–$50.5°$C sensitivity range and a $\pm 1.3°$C propagated error margin. Existing records cannot verify that $50.0°$C occurred in 1977, but such maxima are physically plausible if a 1977-scale event recurs over today's industrial shoreline. In health psychology and occupational medicine, this $+2.08$–$2.8°$C coastal amplification and nocturnal heat ($T_{\min} \approx 30$–$31.4°$C) distort risk perception, degrade neurocognitive vigilance, and increase psychiatric morbidity. Finally, we outline targeted heat-safety updates for Greek authorities and recommend pairing wind-tunnel calibrations with parallel fan-aspirated field trials in WMO record assessments.

1 Introduction

1.1 Geography of West Athens

Defining West Athens in urban climatology requires separating municipal borders from the physical continuum of the Athens Metropolitan Area (Founda et al., 2015; Kassomenos et al., 2003). This distinction is not trivial. The metropolitan region covers $2{,}929$ km^2 across Attica and includes 58 municipalities with over 3.8 million inhabitants (Hellenic Statistical Authority, 2021; Institute of Local Administration, 2010; Salvati, 2014). Under the national numbering plan of the Hellenic Telecommunications and Post Commission (2006), the Athens metropolitan area shares the telephone prefix 21. This dialing zone includes the Thriasio Plain municipalities of Elefsina, Aspropyrgos, Mandra, and Magoula. Administratively, the Kallikratis Programme (Hellenic Parliament, 2010) divides this western territory into two Regional Units separated by Mount Aigaleo (468 m a.s.l.). The Regional Unit of West Athens (*Perifereiaki Enotita Dytikou Tomea Athinon*) occupies the western part of the central Athens Basin, comprising Peristeri, Ilion, Aigaleo, Petroupoli, Chaidari, Agia Varvara, and Agioi Anargyroi-Kamatero. West of Mount Aigaleo lies the Regional Unit of West Attica (*Perifereiaki Enotita Dytikis Attikis*). Its urban-industrial core is the Thriasio Plain (*Thriasio Pedio*, or Thriassion Plain; Hermides et al., 2020; Mavrakis et al., 2012), which encompasses Aspropyrgos, Elefsina, Mandra-Eidyllia, and Fyli (Giannaros et al., 2013; Mavrakis & Papavasileiou, 2013) (Figure 1).

Mesoscale modeling and air-quality studies treat the Thriasio Plain as the western industrial and suburban sector of Greater Athens, calling it the West Athens Metropolitan Sector or simply West Athens (Asimakopoulos et al., 1992; Fameli & Assimakopoulos, 2016; Kassomenos et al., 1995; Tombrou et al., 2007). Although the hydrological catchment covers 500 km^2, industry, housing, and transport are concentrated within a 120 km^2 lowland plain sloping gently (3%) toward the Bay of Elefsis (Mavrakis et al., 2008, 2012). Surveys by the Bureau of Pollution Control and Environmental Quality (BPCEQ) record more than $2{,}200$ industrial and commercial facilities in the basin, including oil refineries, steelworks, cement plants, chemical factories, large warehouse and logistics hubs, 9 quarries, and 13 harbor docks. Narrow passes at Dafni and Ano Liosia–Fyli connect the plain to central Athens, so the two basins interact directly within the metropolitan boundary layer (Batchvarova & Gryning, 1998; Kallos et al., 1993; Melas et al., 1998).

1.2 European Extreme Temperature Hierarchy and Relevance of the Sicilian Dispute

Three historical peaks at or above $47.0°$C anchor the extreme summer climatology of the Thriasio Plain: $48.0°$C at the Elefsina Airport Stevenson screen on July 10, 1977, $47.5°$C at the Aspropyrgos Municipality GER station on June 26, 2007, and $47.0°$C in the Elefsina Hydroscope archive on July 19, 1973. On July 10, 1977, strong Saharan advection and prefrontal westerly

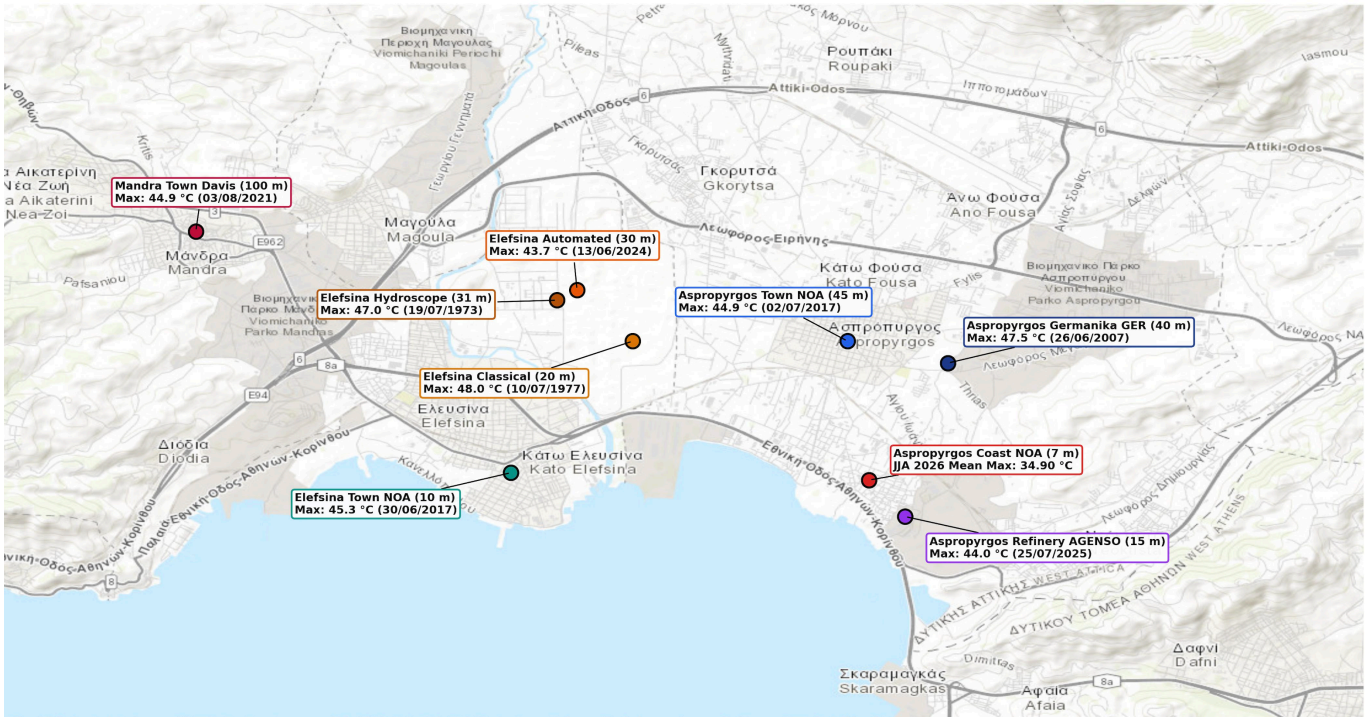


Figure 1: Topographic map of West Athens (Thriasio Plain), showing the locations of the analyzed meteorological stations and their recorded maximum temperatures (or JJA 2026 mean maximum for Aspropyrgos Coast NOA).

to northwesterly katabatic winds drove the official Stevenson screen of the Hellenic National Meteorological Service (HNMS) at Elefsina Airport, as well as the Tatoi HNMS station in the northern Athens Basin, to 48.0°C (118.4°F) (Giles & Balafoutis, 1990; Karatarakis, 2017; Tselepidaki et al., 1995). That reading stood for over four decades as the official European record recognized by the WMO (Cerveny et al., 2007; WMO, 2023).

On August 11, 2021, an automated station operated by the Sicilian Agrometeorological Information Service (SIAS) in Contrada Monasteri, Floridia (Syracuse, Sicily, Italy), registered 48.8°C (119.8°F). A WMO evaluation panel ratified the value following wind-tunnel calibrations at the Italian National Institute of Metrological Research (INRiM), superseding the 1977 Greek record under the WMO Region VI "Europe (continental)" category that groups Mediterranean islands with the mainland (Merlone et al., 2024; WMO, 2023, 2024). The 48.0°C Greek mark was logged simultaneously inside manned HNMS Stevenson screens at two separate airfields (Elefsina and Tatoi) and remains the official European mainland record.

Co-author A. Grassi (Grassi, 2024) tested the passive SIAS multi-plate screen during a 71-day parallel field campaign at Contrada Monasteri (July–September 2024), comparing it against an open-field Barani MeteoHelix sensor at 500 m and a fan-aspirated Tinytag Plus 2 logger at 50 m. Across all 71 days, the SIAS unit recorded higher daily maxima than the Barani sensor by +1.60°C on average, with differences reaching +2.1–3.1°C during sunny afternoon wind lulls of 4–6 km h^{-1} or less. The August 11, 2021 peak coincided with light winds near 5 km h^{-1} inside a screen with a damaged louver 11 m from an asphalt road; on that basis, Grassi (2024) attributed roughly 3°C of the reading to microscale radiative heating, whereas the formal WMO ratification remains in place (Merlone et al., 2024; WMO, 2024). Media reports (MeteoWeb, 2025; Raso, 2026) note that this dispute has also led to administrative legal proceedings before the Regional Administrative Court of Piedmont (TAR Piemonte) against the Italian National Institute of Metrological Research (INRiM) over access to validation documents. Regional readings above 48.0°C have also been logged by the Regional Environmental Protection Agency of Sardinia (ARPA Sardegna), reaching 48.4°C at Orani in 2026 and 48.2°C at Jerzu and Lotzorai in 2023. All three Sardinian measurements came from passive, naturally ventilated shields and remain unconfirmed by the WMO, so they require the same parallel in-situ validation checks. We use these cases strictly as a methodological control for West Athens. In Sections 3.2, 4.2, and 6.2, we test whether the Thriasio Plain extremes reflect calm-wind passive-shield heating or mechanically mixed katabatic flow (15–30 km h^{-1}) inside fan-aspirated shields.

1.3 Historical Extremes in Thriasio Plain

Over the past five decades, stations in the Thriasio Plain have repeatedly logged daily maxima $\geq$ 44.0°C (Table 1; Figure 1). Homogenized normals from the HNMS Climatology Division (Karatarakis, 2017, Table 2) put the reference mean daily maximum at Elefsina Airport (WMO 16718) at 30.7°C in June and 33.3°C in July for 1961–1990, rising to 31.1°C in June and 33.5°C in July for 1971–2000. Four years before the 48.0°C peak of July 10, 1977, on July 19, 1973, the classical Elefsina HNMS Stevenson screen recorded its second-highest maximum of 46.4°C (Karatarakis, 2017). That same afternoon, the digitized half-hourly series in the National Data Bank for Hydrological and Meteorological Information (Hydroscope; HNMS, 1997) registered a plateau of 47.0°C between 13:30 and 14:00 EET. During the late-1980s heatwaves, Elefsina Airport reached 45.0°C on July 23, 1987, 45.2°C on July 27, 1987, and 45.0°C on July 3, 1988 (Giles & Balafoutis, 1990; Prezerakos,

Table 1: Rank-Ordered Inventory of Direct Observations of Extreme Daily Maximum Temperatures (≥ 44.0°C) at Official, Institutional, Davis, and Auxiliary Stations in West Athens (Thriasio Plain, 1973–2025)

Date	Meteorological Station	Operating Authority	Elev. (m)	T_{max} (°C)	Synoptic Regime & Archival Verification
10/07/1977	Elefsina Airport (LGEL)	HNMS Synoptic	20	48.0	Former WMO European Record; All-Time European Mainland Record (W/NW Foehn)
26/06/2007	Aspropyrgos Germanika (GER)	Municipality of Aspropyrgos	40	47.5	Theodor Friedrichs 3030.1000 Fan-Aspirated Pt100 (Mavrakis et al., 2012)
19/07/1973	Elefsina (Station ID 20072)	HNMS Hydroscope Archive	31	47.0	Historical Data Bank (TS 120, Instr. 2007202, 13:30 to 14:00 EET; HNMS, 1997)
19/07/1973	Elefsina Airport (LGEL)	HNMS Synoptic	20	46.4	Classical Stevenson screen maximum thermometer (Karatarakis, 2017)
24/06/2007	Elefsina Airport (LGEL)	HNMS Synoptic	20	45.8	Third-highest historical maximum at LGEL (Karatarakis, 2017)
26/06/2007	Elefsina Airport (LGEL)	HNMS Synoptic	20	45.6	Intense westerly downslope flow across Mount Pateras
30/06/2017	Elefsina Town	NOA Official	10	45.3	Recorded at 16:30 EET under WNW Foehn flow (min RH 12%)
27/07/1987	Elefsina Airport (LGEL)	HNMS Synoptic	20	45.2	Culmination of the deadly July 1987 heatwave (Prezerakos, 1989)
25/07/2007	Elefsina Airport (LGEL)	HNMS Synoptic	20	45.2	Northerly katabatic surge across Mount Parnitha (Karatarakis, 2017)
03/08/2021	Mandra Interchange (Komvos)	NOA/IAASARS OpenHI	61	45.2	Auxiliary hydrological station (passive shield, 15:00 EET; OpenHI, 2026d)
03/08/2021	Gyra Stefanis (North Magoula)	NOA/IAASARS OpenHI	157	45.2	Auxiliary hydrological station (passive shield, northernmost Elefsina, 17:00 EET; OpenHI, 2026a)
23/07/1987	Elefsina Airport (LGEL)	HNMS Synoptic	20	45.0	First major heatwave peak of July 1987 (Giles et al., 1990)
03/07/1988	Elefsina Airport (LGEL)	HNMS Synoptic	20	45.0	Saharan ridge advection and subsidence (Giles & Balafoutis, 1990)
27/06/2007	Elefsina Airport (LGEL)	HNMS Synoptic	20	45.0	Third day ≥ 45.0°C within a four-day span (June 24–27, 2007) at Elefsina Airport
23/07/2023	Mandra Interchange (Komvos)	NOA/IAASARS OpenHI	61	45.0	Auxiliary hydrological station (passive shield, 15:00 EET; OpenHI, 2026d)
02/07/2017	Aspropyrgos Town	NOA Official	45	44.9	Recorded at 14:50 EET under W katabatic flow (daily mean 37.1°C)
03/08/2021	Mandra Town	Davis Station Archive	100	44.9	Davis Vantage Vue (Dioletis, 2021); 15:20 EET under NW Foehn (mean 36.8°C)
03/08/2021	Mandra Diversion (Ektropi)	NOA/IAASARS OpenHI	118	44.9	Auxiliary hydrological station (passive shield, 15:00 EET; OpenHI, 2026c)
30/06/2017	Elefsina Airport (LGEL)	HNMS Synoptic	20	44.8	Simultaneous with 45.3°C at Elefsina Town NOA (Karatarakis, 2017)
03/08/2021	Elefsina Airport (LGEL)	HNMS Synoptic	20	44.8	Peak of the historic August 2021 heatwave under 332° NW wind
03/08/2021	Aspropyrgos Town	NOA Official	45	44.8	Recorded at 14:20 EET under NW katabatic flow (daily mean 36.3°C)
23/07/2023	Elefsina Town	NOA Official	10	44.8	Recorded at 17:00 EET (min RH 16%); +0.8°C over Elefsina Airport
30/06/2017	Aspropyrgos Town	NOA Official	45	44.6	Recorded at 16:10 EET during the June 2017 extreme event
26/07/2023	Mandra Interchange (Komvos)	NOA/IAASARS OpenHI	61	44.6	Auxiliary hydrological station (passive shield, 14:00 EET; OpenHI, 2026d)
26/06/2007	Ergatikes Katikies Mandras (EKM)	BPCEQ Thriasio	50	44.5	Western industrial edge of Elefsina (Mavrakis et al., 2012, Table 3)
26/07/2023	Mandra Diversion (Ektropi)	NOA/IAASARS OpenHI	118	44.5	Auxiliary hydrological station (passive shield, 14:45 EET; OpenHI, 2026c)
23/07/2023	Mandra Diversion (Ektropi)	NOA/IAASARS OpenHI	118	44.4	Auxiliary hydrological station (passive shield, 14:30 EET; OpenHI, 2026c)
02/07/2017	Elefsina Town	NOA Official	10	44.2	Recorded at 13:40 EET (min RH 10%) prior to weak bay breeze
26/06/2007	Paralia Aspropyrgou (P.As)	BPCEQ Thriasio	2	44.0	Heavy industrial coastal zone, 400 m from sea (Mavrakis et al., 2012)
23/07/2023	Elefsina Airport (LGEL)	HNMS Synoptic	20	44.0	Peak of the July 2023 heatwave; Aspropyrgos Town reached 43.9°C
25/07/2025	Aspropyrgos Refinery	AGENSO Network	15	44.0	Pure NW (333°, 15 km h^{-1}) katabatic flow (+2.6°C over Elefsina Classical)

1989).

Severe heatwaves returned in June and July 2007 (Founda & Giannakopoulos, 2009; Theoharatos et al., 2010). In summer 2007, Elefsina Airport reached or exceeded 45.0°C on four days: 45.8°C on June 24 (its third-highest reading on record), 45.6°C on June 26, 45.0°C on June 27, and 45.2°C on July 25 (Founda & Giannakopoulos, 2009; Karatarakis, 2017). On June 26, 2007, hourly observations across seven sites in the Thriasio Plain (Mavrakis et al., 2012) peaked at 47.5°C at the Germanika (GER) municipal station of Aspropyrgos, located 2,500 m inland and less than 2 km from the town center before its 2012 relocation to Alonistra. That same afternoon, BPCEQ stations closer to the coast logged 44.5°C at Ergatikes Katikies Mandras, 600 m inland, and 44.0°C at Paralia Aspropyrgou, 400 m from the sea. Station records from the Municipality of Aspropyrgos, provided via email by Dr. Anastasios Mavrakis (A. Mavrakis, personal communication, August 1, 2, and 7, 2022), show that the Germanika (GER) site used a Theodor Friedrichs Type 3030.1000 transmitter with a 4-wire Pt100 sensor inside a white multi-plate shelter with continuous electrical fan aspiration (Theodor Friedrichs & Co., 1999). On the same day, the official HNMS automated station in Nea Filadelfeia (WMO 16791) also reached 47.5°C, while the co-located classical HNMS Stevenson screen (WMO 16701) read 46.2°C (+1.3°C difference; Karatarakis, 2017, Table 2; Meteoclub, 2013). Across European national meteorological records, this 47.5°C peak logged simultaneously at Aspropyrgos GER (Mavrakis et al., 2012) and Nea Filadelfeia HNMS (Karatarakis, 2017) represents the highest June temperature recorded in Europe, exceeding the national June records of Italy, Portugal, France, and Spain (AEMET, 2025; APAT, 2008; IPMA, 2025; Météo-France, 2020). Neighboring HNMS automated stations in the Regional Unit of West Athens recorded 45.9°C at Ilion (WMO 16788) and 44.1°C at Dafni (WMO 16784; Karatarakis, 2017, Table 2). Since 2014, the automatic weather station network of the NOA (Lagouvardos et al., 2017), local Davis stations (Dioletis, 2021), and the AGENSO telemetry network have captured additional ≥ 44.0°C episodes during the heatwaves of June–July 2017, August 2021 (Founda et al., 2022), July 2023, and July 2025 (Table 1).

1.4 The July 1977 Extreme Event

The synoptic setup of Sunday, July 10, 1977, produced the European mainland record of 48.0°C. A deep subtropical ridge advected a Saharan air mass (850 hPa temperatures above +28–30°C) ahead of an approaching cold front, driving prefrontal westerly and northwesterly Foehn winds across the leeward basins of Attica and Thessaly (Metaxas & Kallos, 1980; Tselepidaki et al., 1995). Duty meteorologist Nikos Kanteres verified the official 48.0°C reading on shift at Elefsina Airport, while the Tatoi HNMS screen hit the same mark (Kolydas, 2023). Two days later, national newspapers (Kathimerini, 1977; Macedonia, 1977a, 1977b; Rizospastis, 1977) and subsequent archival notes (Meteology.gr, 2022) reported five additional unconfirmed readings between 48.0°C and 49.0°C across Greece (Table 2). Their immediate publication across the national press warrants archival investigation to determine whether original paper observation logs were misplaced or omitted when historical HNMS records were digitized.

Table 2: Unconfirmed Extreme Maximum Temperature Reports (≥ 48.0°C) on July 10, 1977 Requiring Archival Investigation

Location / Station	Station Network	T_{max} (°C)	Archival / Press Source
Almyros (Thessaly)	HNMS	49.0	Kathimerini (1977); Macedonia (1977a, 1977b)
Tatoi (Attica)	Likely NOA	48.7	Meteology.gr (2022) archival report
Volos (Thessaly)	HNMS	48.0	Kathimerini (1977); Rizospastis (1977)
Velestino (Thessaly)	HNMS / Agr. Net.	48.0	Kathimerini (1977); Macedonia (1977b)
Messara (Crete)	HNMS / Agr. Net.	48.0	Kathimerini (1977); Macedonia (1977b)

A forest fire also broke out on July 10, 1977, in the northern Athens Basin, burning Aleppo pine and evergreen broadleaves in the area. Forestry Directorate records compiled by Mount Parnitha Forestry Director Georgios Zareifis place the fire's closest approach to Tatoi Airport at roughly 2 km (Kolydas, 2023). Tatoi Airport spans roughly 2 km north to south by 600 m east to west, and the fire never entered the airfield perimeter. Field measurements and heat-transfer models of wildland fires show that radiant heating ahead of a flame front decays within 4–10 flame heights, or less than 50–200 m even for 20 m crown flames (Butler, 2014). Buoyant plume liftoff and turbulent entrainment also dilute convective heat rapidly with distance. During the FireFlux experiment, the upwind surface station remained thermally undisturbed just 100 m from the fire line (Clements et al., 2007; Potter, 2012). Neither the Tatoi Airport HNMS Stevenson screen, 2 km from the fire front, nor the Elefsina Airport screen, 23 km away behind Mount Parnitha and Mount Aigaleo, could have been warmed by the northern Athens Basin fire. At Elefsina Airport, the HNMS hourly log verified by Kanteres shows westerly surface winds (270° W), placing the airfield upwind of the fire (Kolydas, 2023). Archival METAR logs from Elefsina Airport (LGEL) for July 10, 1977, show that during the afternoon peak, surface winds veered to 290°–300° (WNW–NW) at 18–27 km h^{-1} (10–15 kt). That wind sector established a direct overland fetch from the Thriasio foothills across the industrial corridor to the Aspropyrgos coast, blocking the bay breeze.

2 Data and Methodology

2.1 Observational Network

We compiled daily maximum temperature series from nine monitoring sites along the Elefsina–Aspropyrgos–Mandra corridor (1973–2026; Table 3 and Figure 1). Three HNMS stations sit inside the perimeter of Elefsina Airport (LGEL): the classical Stevenson screen (WMO `16718`), the archival Hydroscope station, and the automated Microstep-MIS unit (Station `112`). Outside the airfield, the inland and urban baseline comprises Elefsina Town NOA, Aspropyrgos Town NOA, the Germanika municipal station, and Mandra Town Davis (Dioletis, 2021). Aspropyrgos Town NOA was operated by Th. Geordamilis as telemetry station `SV1EJD` until December 2014. The eastern littoral industrial zone is monitored by Aspropyrgos Coast NOA and Aspropyrgos Refinery AGENSO. Four of these stations are registered with WIGOS identifiers in the WMO OSCAR/Surface repository (Table 4; Lagouvardos et al., 2017; NOA, 2026; WMO OSCAR/Surface, 2026a, 2026b, 2026c, 2026d). For auxiliary inland context, we also checked four NOA/IAASARS hydrological stations: Gyra Stefanis (North Magoula) at the northernmost inland edge of Elefsina Municipality, Mandra Interchange (Komvos), Mandra Diversion (Ektropi), and Mandra Stream (Rema) (OpenHI, 2026a, 2026b, 2026c, 2026d). These hydrological units use passive shields, lack WIGOS registration, and sit over stream channels or road culverts. We therefore exclude them from our spatial transfer equations.

At Elefsina Airport (LGEL), the classical wooden Stevenson screen (WMO `16718`) and the automated station (HNMS Station `112`) operate side by side. Daily SYNOP/BUFR maxima for the Stevenson screen were retrieved for June–July 2017, August 2021, July 2023, and the summers of 2024–2026, yielding 399 summer days in total. Both Elefsina Town NOA and Aspropyrgos Town NOA have complete records across all 399 days. For Elefsina Automated, validated decimal maxima for summer 2026 come from the national open data portal (Hellenic Republic Open Data Portal, 2026). Before that feed launched, daily maxima for 2024 and 2025 were logged daily in real time from the official HNMS telemetry graphs across 172 available days, with 12 missing days in June and August 2024 (Douros, 2026). Those 2024–2025 graphs plotted discrete 30-minute steps rather than continuous peaks, underestimating true daily maxima by about 0.3°C. Sub-hourly logger files from Aspropyrgos Coast across 118 complete summer days confirm a 0.30°C median and 0.34°C mean 30-minute sampling bias (WeatherLink, 2026). Together, the 172 days of 2024–2025 and the 92 decimal days of 2026 form a paired sample of 264 days against Elefsina Classical. The Aspropyrgos Refinery series spans 246 summer days from July 2024 to August 2026, likewise logged daily from the live AGENSO portal (AGENSO, 2026; Douros, 2026). Lastly, 10-minute WeatherLink exports for Aspropyrgos Coast NOA (WeatherLink, 2026) cover 28 days in August 2025, with August 1–3 supplemented from Aspropyrgos Refinery, plus all 92 days of JJA 2026. During a telemetry dropout on June 8–9, 2026, the coastal sensor logged the June 9 peak of 33.9°C at 16:20–16:30 EET under a frozen clock prior to resynchronizing at 17:50 EET. Only June 8 required filling from the adjacent Refinery.

Table 3: Metadata of Analyzed Stations in West Athens

Station	Provider	Lat.	Lon.	Elev.	Coast Dist. / Sensor
Elefsina Classical	HNMS	38.060000	23.560000	20 m	1,450 m / Stevenson
Elefsina Automated	HNMS	38.067000	23.552220	30 m	2,350 m / Microstep
Elefsina Hydroscope	HNMS	38.065600	23.549430	31 m	2,250 m / Archival
Elefsina Town	NOA	38.044738	23.540392	10 m	450 m / Davis Fan
Aspropyrgos Town	NOA	38.063925	23.587953	45 m	2,650 m / Davis Fan
Aspropyrgos GER	Municipality	38.057000	23.604000	40 m	2,500 m / Friedrichs Fan
Aspropyrgos Refinery	AGENSO	38.036000	23.598000	15 m	750 m / Automated
Aspropyrgos Coast	NOA	38.041028	23.592667	7 m	627 m / Davis Fan
Mandra Town	Davis Network	38.075000	23.499000	100 m	4,800 m / Davis Vue

Table 4: Official WMO OSCAR/Surface Registration, Coordinates, and WMO Siting Classifications for the Four Registered Stations in West Athens

OSCAR Name	WIGOS Identifier	Coordinates	Elev.	Siting
Aspropirgos-paralia	`0-300-1-aspropirgospara`	38.041028°N, 23.592667°E	7 m	Class 1
Aspropirgos	`0-300-1-aspropirgos`	38.063925°N, 23.587953°E	45 m	Class 1
Elefsina	`0-300-1-elefsina`	38.044738°N, 23.540392°E	10 m	Class 2
ELEFSIS (AIRPORT)	`0-20000-0-16718`	38.06°N, 23.56°E	20 m	Synoptic

2.2 Physical and Statistical Formulation

Six physical and statistical relations govern our analysis. Air masses descending from the surrounding mountain rim (1,016–1,413 m) warm at the Dry Adiabatic Lapse Rate (Γ_d):

$$\Gamma_d = \frac{g}{c_p} = 9.8\ \mathrm{K\ km^{-1}} \implies \Delta T_{\mathrm{adiab}} = \Gamma_d\,(z_1 - z_2) \quad (1)$$

Between Aspropyrgos Town (45 m) and Aspropyrgos Coast (7 m), Equation 1 gives $\Delta T_{\mathrm{adiab}} = +0.37$°C, or +0.8–1.1°C within a diurnally superheated surface layer ($\Gamma_{\mathrm{eff}} \approx$ 20–30 K $\mathrm{km^{-1}}$; Oke, 1987; Stull, 1988). Across an industrial fetch L with mean wind speed $\overline{u}$ and internal boundary-layer depth $h_{\mathrm{IBL}}(L)$, radiatively driven surface

sensible heat flux $Q_{H,\mathrm{ind}}(x)$ and direct anthropogenic sensible heat release from industrial stacks and process units $Q_{F,\mathrm{ind}}(x)$ accumulate as (Garratt, 1990; Oke et al., 2017):

$$\Delta T_{\mathrm{adv}}(L) = \frac{1}{\rho c_p \overline{u} h_{\mathrm{IBL}}(L)} \int_0^L \left(Q_{H,\mathrm{ind}}(x) + Q_{F,\mathrm{ind}}(x)\right) dx \tag{2}$$

The damping of convective plumes of period P_t and amplitude A_T by a sensor-shield assembly with time constant τ yields a measured amplitude $A_{\mathrm{meas}}(\tau)$ that follows (Hubbard et al., 2001; Lacombe et al., 2011; Nakamura & Mahrt, 2005; WMO, 2018):

$$\frac{A_{\mathrm{meas}}(\tau)}{A_T} = \frac{1}{\sqrt{1 + \left(2\pi\tau / P_t\right)^2}} \tag{3}$$

Serial correlation in consecutive daily residuals $d_i = T_{\mathrm{max},Y,i} - T_{\mathrm{max},X,i}$ is accounted for using the lag-1 autocorrelation coefficient ρ_1 (Zwiers & von Storch, 1995):

$$N_{\mathrm{eff}} = N\,\frac{1-\rho_1}{1+\rho_1}, \quad SE_{\mathrm{adj}} = \frac{s_\Delta}{\sqrt{N_{\mathrm{eff}}}} \tag{4}$$

To obtain the conditional scenario estimator, we restrict the spatial transfer offset to katabatic wind regimes $\theta \in \Omega_{\mathrm{kat}}$ on extreme heatwave days ($T_{\mathrm{max}} \geq 40\,^\circ\mathrm{C}$) and subtract the measured fan-aspirated versus Stevenson offset ΔT_{inst}:

$$\hat{T}^{\mathrm{adj}}_{\mathrm{max},Y} = T^{\mathrm{ref}}_{\mathrm{max},X} + \overline{\Delta T}_{Y-X}\Big|_{\substack{\theta \in \Omega_{\mathrm{kat}} \\ T_{\mathrm{max}} \geq 40\,^\circ\mathrm{C}}} - \Delta T_{\mathrm{inst}} \tag{5}$$

To evaluate conditional uncertainty around Equation 5, we combine four error terms: reference thermometer uncertainty $\sigma_{\mathrm{ref}} = 0.20\,^\circ\mathrm{C}$, residual shield uncertainty $\sigma_{\mathrm{inst}} = 0.25\,^\circ\mathrm{C}$, an uncalibrated structural extrapolation and land-use term $\sigma_{\mathrm{ext}} = 0.50\,^\circ\mathrm{C}$, and the station-specific katabatic transfer error σ_Δ. At the coast, σ_Δ equals $SE_{\mathrm{kat}} = 0.28\,^\circ\mathrm{C}$ for the conditional mean scenario, or $s_{\mathrm{kat}} = 0.79\,^\circ\mathrm{C}$ for a single day:

$$\sigma_{\mathrm{tot}} = \sqrt{\sigma^2_{\mathrm{ref}} + \sigma^2_\Delta + \sigma^2_{\mathrm{inst}} + \sigma^2_{\mathrm{ext}}} \tag{6}$$

At the coastal nodes, Equation 6 gives $\sigma_{\mathrm{tot,mean}} = \pm 0.66\,^\circ\mathrm{C}$, corresponding to a $\pm 1.3\,^\circ\mathrm{C}$ margin at 1.96σ for the conditional mean scenario, and $\sigma_{\mathrm{tot,pred}} = \pm 0.99\,^\circ\mathrm{C}$, or $\pm 1.9\,^\circ\mathrm{C}$ at 1.96σ for a single day. Here $\sigma_{\mathrm{ext}} = 0.50\,^\circ\mathrm{C}$ is an assigned structural parameter rather than a value empirically calibrated against coastal observations near $50\,^\circ\mathrm{C}$, so these margins depend on the assumed error model and do not represent empirical frequentist coverage bands. Equation 6 also assumes that the four error terms act independently. If shield biases and boundary-layer extrapolation errors covary positively during extreme heat, simple linear summation of $\pm 1.23\,^\circ\mathrm{C}$ provides a more conservative upper bound than quadrature.

3 Results

3.1 The 2012, 2017, 2021, and 2023 Heatwaves

Archived observations from Aspropyrgos Town in summer 2012 show a June monthly mean daily maximum of $34.0\,^\circ\mathrm{C}$ (Douros, 2026). During the 9-day heatwave core of July 8–16, 2012, Aspropyrgos Town averaged $39.96\,^\circ\mathrm{C}$ against $38.76\,^\circ\mathrm{C}$ at Elefsina Classical, a mean excess of $+1.20\,^\circ\mathrm{C}$, with daily excesses reaching $+2.6\,^\circ\mathrm{C}$ on July 14 and $+1.7\,^\circ\mathrm{C}$ on July 15.

Across the 61 days of June and July 2017, simultaneous records from Elefsina Town NOA, Aspropyrgos Town NOA, and Elefsina Classical capture a major $> 45\,^\circ\mathrm{C}$ event. Radiosonde ascents by HNMS at Hellinikon measured 850 hPa temperatures of $26.5\,^\circ\mathrm{C}$ on June 30 and $27.5\,^\circ\mathrm{C}$ on July 1 at 00:00 UTC (Karatarakis, 2017, p. 7). Over the 61 days, Aspropyrgos Town averaged $31.90\,^\circ\mathrm{C}$ in June and $34.71\,^\circ\mathrm{C}$ in July, while Elefsina Town NOA averaged $31.49\,^\circ\mathrm{C}$ in June and $34.65\,^\circ\mathrm{C}$ in July, a two-month mean difference of $+0.23\,^\circ\mathrm{C}$. Across the 3-day peak of June 30 to July 2, 2017, shifting katabatic winds alternated the highest maxima between the western and eastern sectors of the plain. On June 30, 2017, west-northwesterly Foehn gusts of 38.6 km h^{-1} and 12% relative humidity drove Elefsina Town NOA to $45.3\,^\circ\mathrm{C}$ at 16:30 EET. That peak topped Elefsina Classical at $44.8\,^\circ\mathrm{C}$ by $+0.5\,^\circ\mathrm{C}$ and Aspropyrgos Town at $44.6\,^\circ\mathrm{C}$ by $+0.7\,^\circ\mathrm{C}$ (Karatarakis, 2017). On July 1, Aspropyrgos Town hit $41.9\,^\circ\mathrm{C}$ at 13:00 EET versus $40.6\,^\circ\mathrm{C}$ at Elefsina Classical and $39.9\,^\circ\mathrm{C}$ at Elefsina Town NOA. On July 2, westerly downslope winds gusting to 37.0 km h^{-1} pushed Aspropyrgos Town to $44.9\,^\circ\mathrm{C}$ at 14:50 EET, with a 24-hour mean of $37.1\,^\circ\mathrm{C}$ and a daily minimum of $30.6\,^\circ\mathrm{C}$. That mark exceeded Elefsina Town NOA at $44.2\,^\circ\mathrm{C}$ by $+0.7\,^\circ\mathrm{C}$ and Elefsina Classical at $43.8\,^\circ\mathrm{C}$ by $+1.1\,^\circ\mathrm{C}$. Over the 3-day peak, Aspropyrgos Town averaged $43.80\,^\circ\mathrm{C}$, Elefsina Town NOA averaged $43.13\,^\circ\mathrm{C}$, and Elefsina Classical averaged $43.07\,^\circ\mathrm{C}$.

Under prevailing NW winds in August 2021 (Dioletis, 2021), Mandra Town led the network with a monthly mean maximum of $36.35\,^\circ\mathrm{C}$, ahead of Aspropyrgos Town NOA at $35.33\,^\circ\mathrm{C}$ (NNW), Elefsina Classical at $35.25\,^\circ\mathrm{C}$, and bay-exposed Elefsina Town NOA at $35.17\,^\circ\mathrm{C}$ (S). This inland-to-coast spread widened during the August 1–5 heatwave core, when Mandra Town exceeded $41.0\,^\circ\mathrm{C}$ every day and averaged $42.54\,^\circ\mathrm{C}$, compared with $40.98\,^\circ\mathrm{C}$ at Aspropyrgos Town, $40.80\,^\circ\mathrm{C}$ at Elefsina Classical, and $40.04\,^\circ\mathrm{C}$ at Elefsina Town. On the peak afternoon of August 3, 2021, a 332° NW katabatic flow drove Mandra Town to $44.9\,^\circ\mathrm{C}$ at 15:20 EET, while Aspropyrgos Town NOA and Elefsina Classical both reached $44.8\,^\circ\mathrm{C}$. Daily minima remained high at $29.4\,^\circ\mathrm{C}$ in Mandra and $29.6\,^\circ\mathrm{C}$ in Aspropyrgos Town. Elefsina Town NOA peaked early at 12:40 EET at $43.7\,^\circ\mathrm{C}$ before an afternoon southerly bay breeze cooled the waterfront.

In July 2023, persistent heat kept Aspropyrgos Town NOA at or above $32.0\,^\circ\mathrm{C}$ on all 31 days of the month. Its monthly mean maximum of $36.96\,^\circ\mathrm{C}$ topped Elefsina Classical at $36.68\,^\circ\mathrm{C}$ by $+0.28\,^\circ\mathrm{C}$ and Elefsina Town NOA at $36.41\,^\circ\mathrm{C}$ by $+0.55\,^\circ\mathrm{C}$. During the core heatwave (July 13–26, 2023), Aspropyrgos Town topped Elefsina Classical on days with westerly or weak downslope flow, recording $40.9\,^\circ\mathrm{C}$ vs. $40.0\,^\circ\mathrm{C}$ on July 14, $41.7\,^\circ\mathrm{C}$ vs. $41.0\,^\circ\mathrm{C}$ on July 15 (WNW wind), $40.5\,^\circ\mathrm{C}$ vs. $39.2\,^\circ\mathrm{C}$ on July 20, $40.0\,^\circ\mathrm{C}$ vs. $38.6\,^\circ\mathrm{C}$ on July 22, and $42.2\,^\circ\mathrm{C}$ vs. $41.6\,^\circ\mathrm{C}$ on July 26. On the peak day of July 23, 2023, a light easterly wind at the airport (77° E at 10 km h^{-1}) and late-afternoon coastal convergence pushed Elefsina Town NOA to $44.8\,^\circ\mathrm{C}$ at 17:00 EET with 16% minimum relative humidity, exceeding Elefsina Classical at $44.0\,^\circ\mathrm{C}$ by $+0.8\,^\circ\mathrm{C}$ and Aspropyrgos Town at $43.9\,^\circ\mathrm{C}$ by $+0.9\,^\circ\mathrm{C}$.

Table 5: Summer (JJA) Mean Daily Maximum ($T_{\max}$, °C) and Absolute Maximum Temperatures (in parentheses, °C) Across the Elefsina and Aspropyrgos Station Network (2024–2026)

Summer	Meteorological Station (Sensor Type)	June $T_{\max}$ (Abs.)	July $T_{\max}$ (Abs.)	August $T_{\max}$ (Abs.)	JJA Mean $T_{\max}$ (Abs.)
2024	1. Aspropyrgos Town NOA (Davis Fan)	35.35 (40.4)	36.01 (38.9)	35.57 (39.2)	35.64 (40.4)
2024	2. Elefsina Classical HNMS (Stevenson)	35.59 (42.4)	36.28 (39.2)	35.65 (39.4)	35.84 (42.4)
2024	3. Elefsina Town NOA (Davis Fan)	35.51 (40.8)	36.40 (39.3)	35.86 (39.4)	35.92 (40.8)
2024	4. Elefsina Automated HNMS (Microstep)[a]	36.43 (43.7)	36.96 (39.8)	36.42 (40.0)	36.60 (43.7)
2024	5. Aspropyrgos Refinery (AGENSO)[b]	[37.14 est.]	37.65 (41.5)	37.33 (42.4)	37.49 (Jul–Aug obs.)
2024	6. Aspropyrgos Coast NOA (Method C Est.)[c]	37.14 (N/A)	37.83 (N/A)	37.33 (N/A)	37.43 [37.11–37.43]
2025	1. Aspropyrgos Town NOA (Davis Fan)	33.17 (39.2)	35.99 (41.2)	32.88 (36.4)	34.01 (41.2)
2025	2. Elefsina Classical HNMS (Stevenson)	33.73 (39.9)	36.50 (41.8)	33.46 (38.0)	34.56 (41.8)
2025	3. Elefsina Town NOA (Davis Fan)	33.93 (40.4)	36.87 (41.8)	33.58 (36.7)	34.79 (41.8)
2025	4. Elefsina Automated HNMS (Microstep)[a]	34.50 (40.9)	37.30 (42.3)	34.13 (38.3)	35.31 (42.3)
2025	5. Aspropyrgos Refinery (AGENSO)	35.20 (42.2)	37.55 (44.0)	34.48 (37.5)	35.74 (44.0)
2025	6. Aspropyrgos Coast NOA (Davis Fan)[d]	N/A	N/A	35.00 (38.8)	N/A [35.05 Aug]
2026	1. Aspropyrgos Town NOA (Davis Fan)	31.70 (36.3)	33.90 (37.6)	34.70 (38.6)	33.43 (38.6)
2026	2. Elefsina Classical HNMS (Stevenson)	31.93 (36.2)	33.91 (37.4)	34.69 (38.6)	33.51 (38.6)
2026	3. Elefsina Town NOA (Davis Fan)	32.06 (36.3)	34.08 (37.8)	34.77 (38.7)	33.64 (38.7)
2026	4. Elefsina Automated HNMS (Microstep)	33.05 (37.1)	34.95 (38.5)	35.78 (39.8)	34.59 (39.8)
2026	5. Aspropyrgos Refinery (AGENSO)	33.10 (37.9)	34.98 (38.6)	36.05 (39.9)	34.71 (39.9)
2026	6. Aspropyrgos Coast NOA (Davis Fan)[e]	33.48 (38.1)	35.16 (38.4)	36.06 (39.6)	34.90 (39.6)

[a]Archived from HNMS telemetry graphs in 2024 ($n = 80$; normalized June and August means) and 2025 ($n = 92$; Douros, 2026); JJA means are the arithmetic average of monthly means. [b]Operated July 2024–August 2026 ($N = 246$; Douros, 2026). [c]Method C estimate; Methods A–C span 37.11–37.43°C (Section 3.3). [d]August 4–31 ($n = 28$); 35.05°C with August 1–3 filled from Refinery. [e]June 8 filled from Refinery (Section 2.1).

Table 6: Top 10 Hottest Coastal Stations (< 1 km from Sea, < 100 m Elevation) Evaluated in the NOA Network Across Greece (JJA 2026)

Station	Elev. (m)	Dist. (m)	June	July	Aug.	JJA Mean
1. Aspropyrgos Coast	7	627	33.48	35.16	36.06	34.90 °C
2. Loutraki	24	689	32.90	35.58	35.81	34.76 °C
3. Salamina	5	39	33.30	34.68	35.59	34.52 °C
4. Amfilochia	40	94	32.12	34.74	36.12	34.33 °C
5. Foinikas (Kalamaria)	15	732	32.42	35.02	35.39	34.28 °C
6. Lindos	65	241	32.05	35.34	35.44	34.28 °C
7. Vlychada	68	630	32.46	34.33	35.26	34.01 °C
8. Ithaca	7	83	31.75	34.24	35.51	33.83 °C
9. Kiato	15	656	31.74	34.55	35.18	33.82 °C
10. Aigio	37	580	31.77	34.57	35.07	33.80 °C

3.2 Multi-Station Intercomparison (2024–2026)

Table 5 presents the monthly and seasonal (JJA) daily maximum statistics across the six stations in Elefsina and Aspropyrgos for 2024, 2025, and 2026. Each summer, the three baseline stations (Elefsina Town NOA, Elefsina Classical, and Aspropyrgos Town NOA) cluster closely. Their seasonal JJA means fall within 0.28°C in 2024 and 0.21°C in 2026, while stronger Etesian ventilation at the inland town site kept Aspropyrgos Town 0.55–0.78°C cooler than the two Elefsina stations in JJA 2025. Across all three summers of 2024–2026, the mean difference between Elefsina Town NOA and the wooden Stevenson screen at Elefsina Classical is $\overline{\Delta T} = +0.15 \pm 0.49$°C, ranging from $+0.08$°C in JJA 2024 to $+0.23$°C in JJA 2025.

Within the airport perimeter, Elefsina Automated exceeded the co-located Stevenson screen by $\overline{\Delta T} = +0.86 \pm 0.38$°C and Elefsina Town NOA by $+0.71$°C. Its daily offset ranged from 0.0°C to $+2.4$°C with a $+0.80$°C median and zero negative residuals across 264 paired days. In 2024 and 2025, the seasonal offset over Elefsina Classical averaged $+0.75$°C and $+0.74$°C. In JJA 2026, it rose to $+1.08$°C in the continuous decimal government feed, reflecting the 0.3°C resolution gap between the 2024–2025 discrete telemetry graphs and the 2026 decimal feed. This $+0.86$°C ($+1.08$°C decimal) offset applies specifically to the co-located Microstep-MIS Pt100 and wooden Stevenson screen pair at Elefsina Airport rather than to automated stations in general.

The highest maxima occur along the Aspropyrgos industrial coast. In August 2025, Aspropyrgos Coast NOA averaged 35.00°C over its 28 operating days and 35.05°C across the full 31-day month, peaking at 38.8°C on August 11. That monthly mean ran $+2.17$°C warmer than Aspropyrgos Town, $+1.59$°C warmer than Elefsina Classical, $+1.47$°C warmer than Elefsina Town NOA, $+0.92$°C warmer than Elefsina Automated, and $+0.57$°C warmer than Aspropyrgos Refinery (Table 5). In JJA 2026, Aspropyrgos Coast NOA logged a seasonal mean daily maximum of 34.90°C, ranking first among all 117 coastal stations within 1 km of the sea and below 100 m elevation in the NOA network across Greece, ahead of Loutraki at 34.76°C (Table 6). Its JJA 2026 mean stood $+1.26$°C above Elefsina Town NOA, $+1.47$°C above Aspropyrgos Town NOA, and $+1.39$°C above Elefsina Classical.

3.3 Summer 2024 Empirical Coastal Estimation

Aspropyrgos Coast NOA began operating in August 2025, so we use three distinct methods to estimate its JJA 2024 seasonal mean, which together span 37.11–37.43°C. In summer 2024, direct observations at Aspropyrgos Town NOA yielded a JJA mean daily maximum of 35.64°C, while Elefsina Town NOA averaged 35.92°C (Table 5). Over the same summer, the ad-

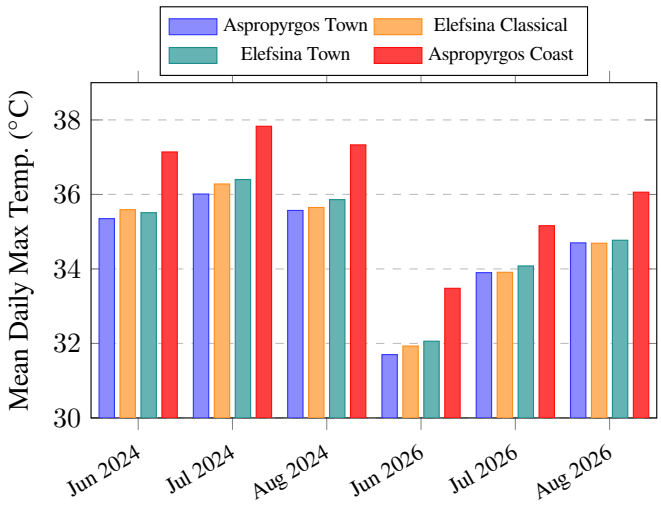


Figure 2: Method C AGENSO-based estimates (2024; full range across Methods A–C is 37.11–37.43°C) and direct observations (2026) of monthly mean daily maximum temperatures (°C) across Aspropyrgos Town NOA, Elefsina Classical Stevenson, Elefsina Town NOA, and Aspropyrgos Coast NOA.

jacent Aspropyrgos Refinery AGENSO station logged monthly mean daily maxima of 37.65°C in July and 37.33°C in August. Method A applies the 2026 monthly differentials from Aspropyrgos Town and Elefsina Town NOA to yield a 2024 JJA mean of 37.11–37.18°C, whereas Method B conditions on the NNW wind regime of July 2024 and gives 37.24°C. Method C, shown in Row 6 of Table 5 and Figure 2, anchors July and August 2024 directly to the co-located Aspropyrgos Refinery observations. For June 2024, triangulating from Elefsina Classical and Aspropyrgos Town yields 37.14°C and 37.13°C, or a three-station mean of 37.07°C if bay-exposed Elefsina Town is included. For July and August 2024, Method C adds the 2026 Coast-minus-Refinery micro-offsets of $+0.18$°C and $< +0.01$°C to the unrounded Refinery means:

$$\begin{aligned} T_{\text{max,Jun 2024}}^{\text{Coast (Method C)}} &\approx 37.14^\circ\text{C}, \\ T_{\text{max,Jul 2024}}^{\text{Coast (Method C)}} &\approx 37.83^\circ\text{C}, \\ T_{\text{max,Aug 2024}}^{\text{Coast (Method C)}} &\approx 37.33^\circ\text{C}, \\ \text{JJA}_{2024}^{\text{Coast (Method C)}} &\approx 37.43^\circ\text{C}. \end{aligned} \tag{7}$$

4 Discussion and Thermodynamic Analysis

4.1 Coastal Thermal Amplification Hypotheses

Aspropyrgos Coast consistently records higher mean and extreme daily maxima than both inland Aspropyrgos Town and waterfront Elefsina Town NOA (Figure 1). Four boundary-layer mechanisms drive this warming across the eastern Thriasio Plain. Basin geometry and bay bathymetry set the baseline. Mountains of 1,000–1,400 m enclose the plain to the north and west, Mount Aigaleo bounds the east, and the 200 m northern ridge of Salamina Island blocks the south (Hermides et al., 2020; Mavrakis et al., 2012). The Bay of Elefsis is a shallow, semi-enclosed lagoon with an 18 m mean depth, and its sheltered northeastern recess off Aspropyrgos warms strongly each summer. Exposure to the sea breeze also differs between the two coastal sites: Elefsina Town faces the wider central bay where southerly winds prevail, whereas southerly flow reaching Aspropyrgos Coast must cross the limestone ridge of Salamina Island.

During Etesian N–NNW or prefrontal W–WNW heatwaves, downslope adiabatic compression warms the air mass further as it descends into the basin (Koletsis et al., 2009; Whiteman, 2000), with Aspropyrgos Coast at 7 m elevation lying 23–93 m lower than the inland stations. Upwind land cover reinforces this warming. Unlike northerly trajectories crossing residential or airfield ground toward Elefsina, NNW–N winds reaching the Aspropyrgos shoreline pass over a 4–6 km refinery and heavy-industry corridor where dry, impervious surfaces partition net radiation Q^* and anthropogenic heat Q_F into sensible heat flux Q_H (Oke et al., 2017; Sailor, 2011). Near the shoreline, offshore katabatic flow also meets the opposing bay-breeze pressure gradient, and the resulting micro-convergence can slow horizontal advection over the heated industrial strip (Melas et al., 1998; Tombrou et al., 2007).

4.2 Katabatic Dynamics (2024–2026)

Table 7 lists the synoptic wind vectors and daily maxima across the network on 19 major heatwave days during 2024–2026. Comparing the dominant wind directions at Elefsina Town NOA and Aspropyrgos Town NOA with Elefsina Airport (LGEL) illustrates how the bay breeze competes with offshore katabatic winds. On June 11 and June 13, 2024, light westerly winds of 5–6 km h^{-1} at Elefsina Airport allowed Elefsina Classical to reach 40.4°C and 42.4°C, while Elefsina Automated hit 41.7°C and 43.7°C. Along the coast, however, an onshore ESE/SSE bay breeze held Elefsina Town NOA to 39.4°C and 40.8°C, with Aspropyrgos Town at 38.4°C and 40.4°C. A similar pattern developed on July 24, 2025. Light northerly flow at the airport pushed Elefsina Classical to 41.8°C and Elefsina Automated to 42.3°C, whereas a SSE bay breeze capped Elefsina Town NOA at 41.6°C and Aspropyrgos Refinery at 40.6°C.

The regime reversed on July 25, 2025, when a 333° NW katabatic flow of 15 km h^{-1} at the airport and N–NNW gusts of 35–40 km h^{-1} across the NOA stations drove the marine boundary layer offshore. While inland and western stations stayed between 41.1°C and 42.3°C, Aspropyrgos Refinery climbed to 44.0°C, standing $+2.9$°C above Aspropyrgos Town, $+2.6$°C above Elefsina Classical, and $+2.2$°C above Elefsina Town NOA (Table 7). Likewise, on August 11, 2025, under a brisk 335° NW Etesian flow of 30 km h^{-1} at the airport, Aspropyrgos Coast reached 38.8°C at 20% relative humidity against 36.4°C at both Aspropyrgos Town and Elefsina Town NOA and 36.0°C at Elefsina Classical, a $+2.8$°C excess. Ten-minute coastal logs show relative humidity dropping to 17–20% during Foehn peaks just 627 m from the shore, whereas sea-breeze days push the coastal Heat Index to 38.9°C and wet-bulb temperatures to 25.3°C (WeatherLink, 2026). Across all 14 days in 2024–2025 when Aspropyrgos Refinery reached or exceeded 40.0°C, its mean excess was $+1.99$°C over the Elefsina Stevenson screen and $+1.86$°C over Elefsina Town NOA. During pure N/NW katabatic peaks, the mean excess reached $+2.08$°C over Elefsina Classical and $+1.93$°C over Elefsina Town NOA.

Table 7: Direct Observations of Synoptic Wind Vectors and Daily Maximum Temperatures (°C) Across the Analyzed Station Network During Peak Heatwave Episodes in West Athens (2024–2026)

Date	LGEL Wind Vector (Dir., Speed)	Elefsina Classical	Elefsina Town NOA	Elefsina Automated	Aspropyrgos Refinery	Aspropyrgos NOA (Coast / Town)	Δ(Auto. − Classical)	Δ(Coast/Ref. −[c] Classical)
11/06/2024	256° W (6 km h^{-1})	40.4	39.4 (ESE)	41.7	N/A	38.4 (Town)	+1.3	N/A
13/06/2024	262° W (5 km h^{-1})	42.4	40.8 (SSE)	43.7	N/A	40.4 (Town)	+1.3	N/A
13/07/2024	3° N (13 km h^{-1})	39.0	38.9 (N)	39.4	40.4	38.4 (Town)	+0.4	+1.4
17/07/2024	351° N (12 km h^{-1})	38.6	38.4 (NNW)	39.2	40.7	38.2 (Town)	+0.6	+2.1
18/07/2024	355° N (17 km h^{-1})	39.2	39.3 (N)	39.8	41.1	38.9 (Town)	+0.6	+1.9
23/07/2024	357° N (10 km h^{-1})	38.4	38.9 (NNW)	38.8	41.5	37.7 (Town)	+0.4	+3.1
16/08/2024	358° N (15 km h^{-1})	39.4	39.4 (N)	40.0	42.4	39.2 (Town)	+0.6	+3.0
17/08/2024	354° N (14 km h^{-1})	37.5	37.4 (NW)	37.8	41.2	37.2 (Town)	+0.3	+3.7
24/08/2024	350° N (10 km h^{-1})	38.4	38.3 (NNW)	N/A	40.8	37.8 (Town)	N/A	+2.4
25/06/2025	357° N (13 km h^{-1})	38.0	38.3 (N)	38.9	40.9	37.6 (Town)	+0.9	+2.9
26/06/2025	357° N (17 km h^{-1})	39.0	39.3 (N)	39.8	40.3	38.4 (Town)	+0.8	+1.3
27/06/2025	358° N (16 km h^{-1})	39.9	40.4 (NNE)	40.9	42.2	39.2 (Town)	+1.0	+2.3
24/07/2025	352° N (10 km h^{-1})	41.8	41.6 (SSE)	42.3	40.6	41.2 (Town)	+0.5	−1.2
25/07/2025	333° NW (15 km h^{-1})	41.4	41.8 (N)	42.3	44.0	41.1 (Town)	+0.9	+2.6
11/08/2025	335° NW (30 km h^{-1})	36.0	36.4 (NNW)	37.2	37.3	38.8 (Coast)[a]	+1.2	+2.8
30/06/2026	355° N (21 km h^{-1})	36.2	36.3 (NW)	37.1	37.9	38.1 (Coast)	+0.9	+1.9
18/07/2026	330° NW (13 km h^{-1})	37.4	37.5 (NW)	38.5	38.6	38.4 (Coast)	+1.1	+1.2
23/08/2026	202° S (8 km h^{-1})	37.4	37.1 (SW)	39.2	39.9	39.6 (Coast)	+1.8	+2.5
24/08/2026	336° NW (20 km h^{-1})	38.6	38.7 (NW)	39.4	39.4	39.6 (Coast)[b]	+0.8	+1.0

[a] +2.4°C over Aspropyrgos Town and +2.8°C over Elefsina Classical. [b] Recorded at 15:20 EET (24-h mean 32.9°C, wind N); +1.0°C over Aspropyrgos Town and Elefsina Classical. [c] Defined as $\max(T_{\text{max,Coast}}, T_{\text{max,Ref.}}) - T_{\text{max,Classical}}$ ($T_{\text{max,Ref.}} - T_{\text{max,Classical}}$ prior to August 2025).

4.3 Biometeorological, Neurocognitive, and Health Psychology Implications

The +2.08°C mean katabatic offset, which reaches +2.8°C on peak days along the Aspropyrgos coast, creates a practical blind spot in local heat-health monitoring (Mavrakis et al., 2012; Theoharatos et al., 2010). Public heat advisories for West Athens rely on the Elefsina Airport Stevenson screen (Karatarakis, 2017), which during downslope Foehn episodes reads 2–3°C cooler than the eastern industrial shoreline. When air temperatures exceed 45.0°C at 10–16% relative humidity (Table 1), ambient air is more than 10°C warmer than the $\sim$ 35°C human skin surface, reversing convective heat transfer so that brisk katabatic winds add sensible heat to the body (Ebi et al., 2021; Giles et al., 1990; Tselepidaki et al., 1995). Experimental work in thermal ergonomics shows that uncompensated heat strain at these levels impairs prefrontal executive control, working memory, sustained vigilance, and reaction time (Hancock & Vasmatzidis, 2003). Within the refinery, warehouse, logistics, and heavy-industry zone of Aspropyrgos (Section 1.1), declining vigilance and executive control during afternoon shifts directly increase the likelihood of operational mistakes and workplace accidents. From a health psychology perspective, behavioral adaptation to extreme heat depends on accurate cognitive threat appraisal, perceived susceptibility, and self-efficacy triggered by localized warnings (Heidenreich & Thieken, 2024). Regional advisories anchored to the cooler airfield screen understate littoral industrial temperatures by 2–3°C, with immediate consequences for public-health warnings. Cooler official forecasts can dull perceived heat risk among workers and residents, delaying hydration pacing, work-rest scheduling, and cooling breaks during peak strain (Ebi et al., 2021; Heidenreich & Thieken, 2024).

High daytime maxima in the basin are frequently accompanied by 24-hour minimum temperatures of 29.6–31.4°C (Section 3.1). Daily minima stayed at 30.8°C at Aspropyrgos Town and 31.4°C at Elefsina Town on July 19, 2024. During the July 25–26, 2025 peak, 24-hour minima reached 31.1–31.3°C at the urban NOA stations, while Aspropyrgos Coast logged a 29.6°C minimum on August 9, 2026. Nighttime temperatures near 30–31°C inhibit the nocturnal core body temperature drop needed to enter slow-wave and REM sleep, disrupting sleep continuity and autonomic recovery (Obradovich et al., 2017). In psychiatric epidemiology, multi-day heatwaves with warm nights are associated with higher rates of emergency psychiatric admissions, mood and psychotic relapses, agitation, and suicidal behavior (Liu et al., 2021; Lõhmus, 2018; Theoharatos et al., 2010). Risk is further elevated in patients taking dopamine-antagonist antipsychotics, anticholinergics, tricyclic antidepressants, or lithium, as these medications suppress hypothalamic thermoregulation and sweating (Lõhmus, 2018) when ambient temperatures climb into the 45.0–50.0°C range.

4.4 Policy and Operational Recommendations for Greek Authorities

These temperature offsets across the eastern industrial zone expose a clear gap in Greek heat-safety rules. Under Presidential Decree 62/2025 and directives from the Hellenic Ministry of Labour and Social Security (2024, 2026), mandatory afternoon work stoppages (12:00–17:00 EET) apply to outdoor construction, shipyards, technical works, and two-wheeled delivery. Yet these suspensions rely on HNMS temperature and Wet-Bulb Globe Temperature (WBGT) forecasts tied to Elefsina Airport. That single-station trigger misses extreme heat in the industrial zone. On 12 of the 14 days in 2024–2025 when the Aspropyrgos

industrial zone reached or exceeded $40.0°$C, the Elefsina screen stayed below $40.0°$C. On August 16, 2024, the industrial zone hit $42.4°$C while the airfield read $39.4°$C; on June 27, 2025, it reached $42.2°$C against $39.9°$C at the airport. Even during the July 25, 2025 peak, the industrial zone reached $44.0°$C while the Elefsina screen recorded $41.4°$C, a $+2.6°$C excess. Dry Foehn winds at 10–20% relative humidity create a second blind spot. Low humidity keeps WBGT modest even when dry-bulb temperatures above $44.0°$C reverse convective heat transfer and impair worker vigilance. For the Thriasio industrial zone, the Ministry of Labour, the Labor Inspectorate, and the HNMS should tie work-stoppage triggers to the WIGOS Class 1 Aspropyrgos Coast NOA station. Where airfield forecasts are used, adding a $+2.0$ to $+2.8°$C katabatic offset under northerly-to-westerly flow and pairing WBGT with strict dry-bulb cutoffs would close this gap. Civil Protection and the HNMS can likewise split West Attica heat advisories and 112 alerts between the western airfield and the eastern industrial zone. At the municipal level, Hellenic Ministry of Health (2026) heatwave guidance should account for warm nights. When 24-hour minima approach 30–$31.4°$C, Aspropyrgos, Elefsina, and Mandra-Eidyllia need 24-hour cooling centers, and local clinics should alert psychiatric outpatients taking antipsychotics, anticholinergics, tricyclic antidepressants, or lithium.

5 Historical Scenarios and Working Hypotheses

5.1 2007 Validation vs. Conditional 1977 and Modern-Climate Scenarios

Transferring extreme temperatures across the Thriasio Plain requires separating three questions. We first test whether modern spatial offsets reproduce an observed historical heatwave (June 26, 2007), then project those differentials onto the July 10, 1977 mainland record, and finally evaluate how a 1977-strength synoptic event would behave over contemporary industrial land cover.

We begin with the June 26, 2007 cross-station check (Table 8). Both criteria governing our modern transfer subsets, namely $T_{\max} \geq 40.0°$C and north-to-northwesterly katabatic wind directions of 330–358°, were locked in *a priori* from synoptic climatology and 2024–2026 wind roses. No 2007 observations were used to tune these bounds. On June 26, 2007, brisk westerly and northwesterly downslope winds drove the classical Elefsina Stevenson screen to $45.6°$C, two days after its $45.8°$C peak on June 24, while the fan-aspirated Pt100 municipal station at Germanika (GER) hit $47.5°$C (Mavrakis et al., 2012), an observed gap of $+1.90°$C. Adding our out-of-sample 2024–2025 extreme differential of $+1.99°$C or the fan-aspirated katabatic differential of $+1.93°$C to the $45.6°$C Elefsina benchmark gives 47.5–$47.6°$C at the current Aspropyrgos Coast NOA site, matching the $47.5°$C municipal Pt100 record within $0.1°$C.

Close agreement at $47.5°$C in 2007, however, does not guarantee that identical spatial gradients held when Elefsina Classical reached $48.0°$C on July 10, 1977, nor does it verify strict linearity near $50°$C. No thermometer operated on the Aspropyrgos waterfront in 1977. Impervious industrial plots upwind of Aspropyrgos Coast have also expanded substantially over the intervening five decades, so reconstructing July 1977 and modeling a future 1977-analog event pose distinct physical questions. Superposing the modern empirical offsets of $+1.39°$C, $+2.08°$C, and $+2.60°$C onto the $48.0°$C Elefsina baseline gives three conditional point estimates at the Aspropyrgos coast:

$$\begin{aligned} T^{\text{cons}}_{\max,1977} &= 48.00°\text{C} + 1.39°\text{C} \approx 49.4°\text{C} \ (\text{Adj.: } 49.2°\text{C}) \\ T^{\text{cent}}_{\max,1977} &= 48.00°\text{C} + 2.08°\text{C} \approx 50.1°\text{C} \ (\text{Adj.: } 49.9°\text{C}) \\ T^{\text{peak}}_{\max,1977} &= 48.00°\text{C} + 2.60°\text{C} = 50.6°\text{C} \ (\text{Adj.: } 50.5°\text{C}) \end{aligned} \tag{8}$$

In Table 8, direct measurements are marked [Obs.] and conditional transfer estimates are marked [Cond.]. For statistical consistency across all rows, the second column of Table 8 reports each station's central katabatic offset followed in parentheses by the empirical wind-regime offset range from the all-summer baseline to the katabatic peak. To maintain comparability with the Elefsina Stevenson screen, the shield-adjusted values apply a station-specific instrumental correction ΔT_{inst} in Equation 5. For the 24-hour fan-aspirated Davis units at Elefsina Town, Aspropyrgos Town, and Aspropyrgos Coast, we subtract the 399-day fan-aspirated versus Stevenson offset of $+0.15°$C. This adjustment shifts the three coastal estimates in Equation 8 from 49.24, 49.93, and $50.45°$C to 49.2, 49.9, and $50.5°$C. We apply $-0.1°$C for the fan-aspirated Friedrichs Pt100 shelter at Aspropyrgos GER and $-0.4°$C for the passive Microstep-MIS shield at Elefsina Automated.

The fifth column of Table 8 shows how the conditional point estimate shifts across the empirical wind-regime offset range prior to adding structural uncertainty. The sixth column applies the $\pm 1.96\sigma_{\text{tot,mean}}$ interval from Equation 6 around each station's shield-adjusted central value. At Station 1, only reference thermometer uncertainty $\sigma_{\text{ref}} = 0.20°$C applies, giving $48.0 \pm 0.4°$C. For Stations 2–6, we combine $\sigma_{\text{ref}} = 0.20°$C, $\sigma_{\text{inst}} = 0.25°$C, and $\sigma_{\text{ext}} = 0.50°$C with each station's transfer standard error σ_{Δ}, which ranges from $0.07°$C at Elefsina Town to $0.28°$C at the coast. This yields propagated margins of $\pm 1.2°$C at the inland nodes and $\pm 1.3°$C at Aspropyrgos GER and Aspropyrgos Coast, corresponding to a 48.6–$51.2°$C coastal interval around the $49.9°$C central estimate (Table 8). Using the single-day katabatic standard deviation $s_{\text{kat}} = 0.79°$C widens the coastal margin to $\pm 1.9°$C, or 48.0–$51.8°$C. Because $\sigma_{\text{ext}} = 0.50°$C is an uncalibrated structural term, these bounds reflect model-conditioned error propagation rather than empirical frequentist confidence bands. While the resulting estimates show that coastal maxima near $50.0°$C lie within physical reach during a future 1977-scale heatwave over modern land use, they do not constitute observational proof that $50.0°$C was reached in 1977.

5.2 Autocorrelation and Statistical Diagnostics

Consecutive daily maxima are serially correlated during multi-day heatwaves, so we evaluated the lag-1 autocorrelation ρ_1 of the daily station differentials d_i before testing the observed 2024–2026 sample means (Equation 4; Table 8). Across the 276 paired summer days of 2024–2026 between Elefsina Town NOA and Elefsina Classical, daily residuals exhibit near-zero serial correlation with $\rho_1 = 0.014$, yielding $N_{\text{eff}} = 268.2$ days and $SE_{\text{adj}} = 0.03°$C. Across the 264 paired days between Elefsina Automated and Elefsina Classical, moderate autocorrelation of $\rho_1 = 0.188$ reduces N_{eff} to 180.5 days and gives

Table 8: Observed Benchmarks ([Obs.]) vs. Conditional Transfer Scenarios ([Cond.]) for June 26, 2007 and July 10, 1977 Across West Athens (°C)

Station / Monitoring Node (West Athens Network)	Katabatic Offset: Mean (Range, °C)[a]	June 26, 2007 Check (°C)	1977-Scale Central (Raw / Shield-Adj.)[b]	Wind-Regime Sensitivity Range (Raw / Adj.)[c]	Conditional Propagated Uncertainty (Adj. Mean)[d]
1. Elefsina Classical (Stevenson)	0.00 (0.00) [Ref.]	45.6 [Obs.]	48.0 / 48.0 [Obs.]	48.0 [Obs.]	47.6 to 48.4 °C (±0.4)
2. Elefsina Town (NOA Davis)	+0.15 (+0.1 to + 0.5)	45.7–46.1 [Cond.]	48.2 / 48.0 [Cond.]	48.1–48.5 / 48.0–48.4 [Cond.]	46.8 to 49.2 °C (±1.2)
3. Elefsina Automated (Microstep)	+0.90 (+0.9 to + 1.3)	46.5–46.9 [Cond.]	48.9 / 48.5 [Cond.]	48.9–49.3 / 48.5–48.9 [Cond.]	47.3 to 49.7 °C (±1.2)
4. Aspropyrgos Town (NOA Davis)	+0.80 (+0.5 to + 1.2)	46.1–46.8 [Cond.]	48.8 / 48.6 [Cond.]	48.5–49.2 / 48.4–49.1 [Cond.]	47.4 to 49.8 °C (±1.2)
5. Aspropyrgos GER (Fan Pt100)	+1.90 (+1.5 to + 1.9)	47.5 [Obs.]	49.9 / 49.8 [Cond.]	49.5–49.9 / 49.4–49.8 [Cond.]	48.5 to 51.1 °C (±1.3)
6. Aspropyrgos Coast / Refinery	+2.08 (+1.4 to + 2.6)	47.5–47.6 [Cond.]	50.1 / 49.9 [Cond.]	49.4–50.6 / 49.2–50.5 [Cond.]	48.6 to 51.2 °C (±1.3)

[a]Central katabatic offset and wind-regime range ($N = 399$ at NOA Town nodes, $N = 264$ at Elefsina Automated, $N = 246$ at Coast/Refinery; Section 5.2). [b]Raw and shield-adjusted values per Equation 5 (Section 5.1). [c]Range across the column 2 offsets (Station 6 2007 check uses the $+1.93$°C and $+1.99$°C coastal estimators). [d]Adjusted central $\pm 1.96\sigma_{\text{tot,mean}}$ per Equation 6 (single-day Station 6 interval: 48.0–51.8°C, ±1.9°C).

$SE_{\text{adj}} = 0.03$°C, with $t_{\text{adj}} = 30.37$ and $p < 10^{-16}$. The 246-day comparison between the Aspropyrgos littoral zone and Elefsina Classical has a sample mean of $\overline{\Delta T} = +1.27$°C and standard deviation $s_\Delta = 1.03$°C, yielding $\rho_1 = 0.050$, $N_{\text{eff}} = 222.5$ days, $SE_{\text{adj}} = 0.07$°C, and $t_{\text{adj}} = 18.48$ ($p < 10^{-16}$). Relative to Elefsina Town NOA over the same 246 days, the Aspropyrgos littoral zone averages $+1.10$°C warmer overall, rising to $+1.86 \pm 0.31$°C across the 14 days at or above 40°C and $+1.93 \pm 0.26$°C during N/NW katabatic peaks.

5.3 Exploratory Working Hypotheses for 50.0 °C

Upper-air radiosonde soundings from Hellinikon during the June 30 to July 2, 2017 heatwave (Karatarakis, 2017, p. 7) provide an empirical baseline for the vertical thermal spread across the basin. During that episode, 850 hPa temperatures of 26.5–27.5°C corresponded to surface maxima of 45.3°C at Elefsina Town NOA and 45.4°C at Nea Filadelfeia HNMS, an 850 hPa-to-surface differential of +17.8–18.8°C. This vertical spread suggests a clear synoptic working hypothesis for a 50.0°C event. If an intense North African ridge (Founda et al., 2022; Prezerakos, 1989) advects a +29.5–31.0°C Saharan air mass at 850 hPa while northwesterly katabatic winds block the bay breeze, surface temperatures along the Aspropyrgos coast could reach 50.0°C. Because the present study is observational, coupled mesoscale and large-eddy simulations (WRF-LES) are needed to test this threshold numerically.

6 Limitations and Methodological Uncertainties

6.1 Record Length, Non-Linear Feedbacks, and Historical vs. Modern Land Use

The newest stations in our network have short operational records compared with the 30-year WMO standard normal period (WMO, 2018). Direct observations from Aspropyrgos Coast NOA span August 2025 and JJA 2026, while the Aspropyrgos Refinery and Elefsina Automated series cover the 2024–2026 summers. Multi-decadal monitoring will be required to test the long-term stability of the spatial offsets across different summer circulation regimes.

Physical and historical limitations also govern any extrapolation of empirical differentials from the observed 38.0–45.6°C reference range into the 48–50.6°C regime. Near 50°C (323.15 K), outgoing longwave radiation $L_\uparrow = \epsilon\sigma T_s^4$ rises by about 7.0 W m^{-2} K^{-1}. Stronger buoyant thermals can deepen the convective mixed layer z_i, entrain cooler air from aloft, and reduce $\Delta T_{\max}$ below the linear katabatic offset (Garratt, 1990; Stull, 1988). Conversely, strong subsidence capping h_{IBL} below 100 m can preserve a steep coastal gradient.

Equally important is the distinction between 1977 and present-day land cover. Although the main oil refineries and steelworks were already active in July 1977, paved industrial and commercial surfaces upwind of Aspropyrgos Coast have expanded over the past five decades (Mavrakis & Papavasileiou, 2013; Mavrakis et al., 2012; Salvati, 2014). That surface expansion increases modern sensible heat advection ΔT_{adv} in Equation 2. For July 10, 1977 itself, less extensive industrial sealing implies that actual coastal temperatures likely fell below the modern central transfer estimate, although the exact historical offset cannot be quantified from available records. Under contemporary surface sealing, by contrast, a recurrence of July 1977 synoptic forcing with 48.0°C at the Elefsina airfield screen could plausibly drive the Aspropyrgos littoral strip to the 50.0°C mark.

6.2 Shielding Contrasts and Proposed In-Situ Field Validation

Radiation-shield geometry, ventilation, and sensor time constants also differ across networks (Blonquist & Bugbee, 2014; Hubbard et al., 2001). At Elefsina Airport, the positive offset of Elefsina Automated ($\tau_A \approx 15$–30 s) relative to Elefsina Classical ($\tau_S \approx 180$–300 s) reflects brief convective plumes damped by the wooden Stevenson screen (Equation 3; Section 3.2). The 10-minute Aspropyrgos Coast logs (WeatherLink, 2026) capture these sub-10-minute plumes directly: daily peak temperatures exceed the corresponding 10-minute interval reading by +0.42°C on average and up to +1.8°C. In naturally ventilated multi-plate shields, radiative errors rise when ambient wind speeds fall below 4 m s^{-1} (Blonquist & Bugbee, 2014; Nakamura & Mahrt, 2005). Below 2 m s^{-1}, radiative warming reaches +0.3–1.0°C over grass (Environmental Biophysics, 2014; Lacombe et al., 2011) and +2.0–3.1°C at sheltered sites (Grassi, 2024). Active fan aspiration prevents calm-wind radiative heat buildup, with replicate fan-aspirated shields

agreeing within $0.05°C$ in summer even below 2 m s^{-1} and at $1{,}000$ W m^{-2} (Blonquist & Bugbee, 2014; see also Lacombe et al., 2011, Section 2.2.1.3b and Annex 9.6). In non-desert urban and industrial settings without blowing-sand clogging, maintained fan-aspirated shields avoid passive-screen overheating. Through the NOANN network of the National Observatory of Athens (Lagouvardos et al., 2017), Greece operates more than 600 WIGOS-registered 24-hour fan-aspirated stations (Davis Vantage Pro2 model 6153). Roof-mounted urban units are placed at the roof edge to avoid summer heating from underlying cement or tiles (Lagouvardos et al., 2017). The close agreement between Elefsina Town NOA and the airport Stevenson screen (Section 3.2) confirms the effectiveness of this siting practice.

Wind-tunnel sensor calibrations verify intrinsic probe accuracy, but they cannot capture site-specific radiative coupling, degraded louvers, or road-heated micro-advection during calm lulls (≤ 5 km h^{-1}). To complement laboratory calibrations in future record adjudications, we propose a three-step in-situ validation framework (the Grassi protocol) as a methodological recommendation:

1. **In-Situ Parallel Field Campaigns:** Candidate extremes recorded inside naturally ventilated shields (including unverified regional readings above $48.0°C$ such as those in Sardinia), at stations lacking WIGOS Class 1–2 certification in WMO OSCAR/Surface, or at WMO Class 3–5 sites would benefit from a 60 to 90 warm-season day in-situ parallel field campaign. This recommendation follows the dual-distance field layout used by Grassi (2024) at Floridia (Section 1.2) and our co-located monitoring at Elefsina.

2. **Fan-Aspirated Reference Benchmarking:** Parallel adjudication arrays should deploy both an actively fan-aspirated platinum resistance or thermistor shield and a certified low-radiation reference shield (e.g., Barani MeteoHelix or WMO Class 1 fan-aspirated standard) to separate fast-response convective peaks from calm-wind enclosure heating.

3. **Wind-Regime Conditioning:** Intercomparison residuals should be stratified by wind speed and direction, isolating ≤ 5 km h^{-1} lulls from > 15 km h^{-1} flow. This tests whether the candidate extreme occurred under brisk, mechanically mixed flow (such as the 15–30 km h^{-1} katabatic peaks of West Athens) or during stagnant radiative conditions prone to road-heated thermal plumes.

Before any formal standardization, the Grassi protocol will require independent field testing and metrological replication across diverse climates.

7 Conclusions

Multi-station observations across the Thriasio Plain show that substantial coastal thermal amplification develops in West Athens during north-to-northwesterly katabatic episodes. When downslope flow weakens or displaces the Bay of Elefsis sea breeze, adiabatic compression combines with sensible heat advection across the 4–6 km upwind refinery belt. This process keeps the eastern industrial shoreline warmer than both inland town stations and the western airfield reference screens.

In interpreting the conditional $49.9°C$ transfer estimate derived from the $48.0°C$ Elefsina record of July 10, 1977, historical reconstruction must be separated from present-day boundary-layer behavior. No station operated on the Aspropyrgos waterfront in July 1977, and industrial surface sealing was less extensive than today; modern spatial offsets alone therefore cannot verify that $50.0°C$ occurred historically. Over the contemporary industrial coastline, however, local maxima approaching $50.0°C$ represent a physically plausible scenario if a 1977-magnitude katabatic heatwave recurs, even though existing station records and transfer equations do not establish that this threshold has already been reached.

These microclimatic differentials also have direct applications in health psychology, cognitive ergonomics, and psychiatric epidemiology. Regional heat warnings rely on the cooler Elefsina airfield screen and understate coastal industrial temperatures by 2–3°C, a bias that can lower perceived heat risk and delay self-protective behavior among refinery, warehouse, logistics, shipyard, and outdoor workers, as well as older adults, chronic-disease patients, and psychiatric outpatients. Tighter physical bounds for both WMO record adjudication and localized public-health warnings will require fan-aspirated reference arrays paired with coupled WRF-LES simulations, boundary-layer profiling, and eddy-covariance flux measurements along the industrial coast.

Data Availability

The compiled daily maximum temperature series for Elefsina Automated, Aspropyrgos Refinery, and Aspropyrgos Town NOA are archived on Figshare at https://doi.org/10.6084/m9.figshare.34875324 (Douros, 2026). The workbook contains the 2024–2026 summer observations and daily differentials, the June–July 2012 archival records, monthly summary statistics, and station metadata supporting Tables 5, 7, and 8. The technical report of the 2024 Floridia parallel monitoring campaign (Grassi, 2024) is archived on Figshare at https://doi.org/10.6084/m9.figshare.34906956. Primary agency feeds for the remaining stations and wind observations are also publicly accessible. Daily SYNOP/BUFR temperature maxima and synoptic wind vectors for Elefsina Classical (WMO 16718) are available at https://www.ogimet.com/ and https://www.meteomanz.com/, and historical 1951–1996 HNMS Hydroscope records (HNMS, 1997) are archived at http://emy.hydroscope.gr/stations/d/20072/. Validated JJA 2026 decimal maxima for Elefsina Automated (HNMS Station 112; Hellenic Republic Open Data Portal, 2026) are available at https://data.gov.gr/dataset/emy-station-112. Monthly summaries and dominant wind directions from NOA for Elefsina Town, Aspropyrgos Town, and Aspropyrgos Coast (NOA, 2026) are archived at https://meteosearch.meteo.gr/data/index.cfm, and 10-minute telemetry for Aspropyrgos Coast (WeatherLink, 2026) is accessible at https://www.weatherlink.com/bulletin/dcb78353-cde7-4b72-b4de-eaff4d0d67ba. Mandra Town Davis summaries (Dioletis, 2021) are available at https://mandra.meteoclub.gr/NOAAMO82021.TXT, live AGENSO telemetry (AGENSO, 2026) at https://temperature.gr/, and auxiliary IAASARS/NOA OpenHI series (OpenHI, 2026a, 2026b, 2026c, 2026d) at https://system.openhi.net/stations/1481/timeseriesgroups/1221/, https://system.openhi.net/stations/8424/,

https://system.openhi.net/stations/8425/, and https://system.openhi.net/stations/8426/timeseriesgroups/888/.

References

Agencia Estatal de Meteorología (AEMET). (2025). *Resumen mensual climatológico: Junio 2025* [Monthly climatological summary: June 2025; In Spanish]. Ministerio para la Transición Ecológica y el Reto Demográfico. https://www.aemet.es/documentos/es/serviciosclimaticos/vigilancia_clima/resumenes_climat/mensuales/2025/res_mens_clim_2025_06.pdf

AGENSO. (2026). *Temperature.gr telemetric meteorological station network*. https://temperature.gr/

Agenzia per la Protezione dell'Ambiente e per i Servizi Tecnici (APAT). (2008). *Gli indicatori del clima in Italia nel 2007* [Climate indicators in Italy in 2007; In Italian] (Anno III). Istituto Superiore per la Protezione e la Ricerca Ambientale (ISPRA). https://scia.isprambiente.it/wp-content/uploads/2024/03/Gli-indicatori-del-clima-in-Italia-nel-2007.pdf

Asimakopoulos, D. N., Deligiorgi, D., Drakopoulos, C., Helmis, C., Kokkori, K., Lalas, D., Sikiotis, D., & Varotsos, C. (1992). An experimental study of nighttime air-pollutant transport over complex terrain in Athens. *Atmospheric Environment. Part B. Urban Atmosphere, 26*(1), 59–71. https://doi.org/10.1016/0957-1272(92)90037-S

Batchvarova, E., & Gryning, S.-E. (1998). Wind climatology, atmospheric turbulence and internal boundary-layer development in Athens during the MEDCAPHOT-TRACE experiment. *Atmospheric Environment, 32*(12), 2055–2069. https://doi.org/10.1016/S1352-2310(97)00422-6

Blonquist, M., & Bugbee, B. (2014, August). Active or passive: The challenge of accurately measuring air temperature. *Meteorological Technology International*, 62–64. https://www.apogeeinstruments.com/content/Blonquist-Bugbee-2014-Meteorological-Technology-International.pdf

Butler, B. W. (2014). Wildland firefighter safety zones: A review of past science and summary of future needs. *International Journal of Wildland Fire, 23*(3), 295–308. https://doi.org/10.1071/WF13021

Cerveny, R. S., Lawrimore, J., Edwards, R., & Landsea, C. (2007). Extreme weather records: Compilation, adjudication, and publication. *Bulletin of the American Meteorological Society, 88*(6), 853–860. https://doi.org/10.1175/BAMS-88-6-853

Clements, C. B., Zhong, S., Goodrick, S., Li, J., Potter, B. E., Bian, X., Heilman, W. E., Charney, J. J., Perna, R., Jang, M., Lee, D., Patel, M., Street, S., & Aumann, G. (2007). Observing the dynamics of wildland grass fires: FireFlux—A field validation experiment. *Bulletin of the American Meteorological Society, 88*(9), 1369–1382. https://doi.org/10.1175/BAMS-88-9-1369

Dioletis, N. (2021). *Mandra Davis automatic weather station climatological archive* [Data set]. Meteoclub. https://mandra.meteoclub.gr/NOAAMO82021.TXT

Douros, P. (2026). *Daily summer maximum temperatures (JJA 2024–2026) at Elefsina Automated (HNMS Station 112), Aspropyrgos Refinery (AGENSO), and Aspropyrgos Town NOA (2012) in West Athens, Greece* [Data set]. Figshare. https://doi.org/10.6084/m9.figshare.34875324

Ebi, K. L., Capon, A., Berry, P., Broderick, C., de Dear, R., Havenith, G., Honda, Y., Kovats, R. S., Ma, W., Malik, A., Morris, N. B., Nybo, L., Seneviratne, S. I., Vanos, J., & Jay, O. (2021). Hot weather and heat extremes: Health risks. *The Lancet, 398*(10301), 698–708. https://doi.org/10.1016/S0140-6736(21)01208-3

Environmental Biophysics. (2014). *The quest for accurate air temperature (Part 2)*. https://environmentalbiophysics.org/the-quest-for-accurate-air-temperature-part-2/

Fameli, K. M., & Assimakopoulos, V. D. (2016). The new open Flexible Emission Inventory for Greece and the Greater Athens Area (FEI-GREGAA): Account of pollutant sources and their importance from 2006 to 2012. *Atmospheric Environment, 137*, 17–37. https://doi.org/10.1016/j.atmosenv.2016.04.004

Founda, D., & Giannakopoulos, C. (2009). The exceptionally hot summer of 2007 in Athens, Greece: A typical summer in the future climate? *Global and Planetary Change, 67*(3–4), 227–236. https://doi.org/10.1016/j.gloplacha.2009.03.013

Founda, D., Katavoutas, G., Pierros, F., & Mihalopoulos, N. (2022). The extreme heat wave of summer 2021 in Athens (Greece): Cumulative heat and exposure to heat stress. *Sustainability, 14*(13), Article 7766. https://doi.org/10.3390/su14137766

Founda, D., Pierros, F., Petrakis, M., & Zerefos, C. (2015). Interdecadal variations and trends of the urban heat island in Athens (Greece) and its response to heat waves. *Atmospheric Research, 161–162*, 1–13. https://doi.org/10.1016/j.atmosres.2015.03.016

Garratt, J. R. (1990). The internal boundary layer: A review. *Boundary-Layer Meteorology, 50*(1–4), 171–203. https://doi.org/10.1007/BF00120524

Giannaros, T. M., Melas, D., Daglis, I. A., Keramitsoglou, I., & Kourtidis, K. (2013). Numerical study of the urban heat island over Athens (Greece) with the WRF model. *Atmospheric Environment, 73*, 103–111. https://doi.org/10.1016/j.atmosenv.2013.02.055

Giles, B. D., & Balafoutis, C. J. (1990). The Greek heatwaves of 1987 and 1988. *International Journal of Climatology, 10*(5), 505–517. https://doi.org/10.1002/joc.3370100507

Giles, B. D., Balafoutis, C. J., & Maheras, P. (1990). Too hot for comfort: The heatwaves in Greece in 1987 and 1988. *International Journal of Biometeorology, 34*(2), 98–104. https://doi.org/10.1007/BF01093455

Grassi, A. (2024). *Report on the parallel temperature monitoring carried out in the period between 12/07/24 and 20/09/24, near the regional weather station "SIAS Siracusa", Municipality of Floridia (SR)* (Technical Report, Catania, November 3, 2024; digitally signed November 18, 2024, 22 pp.). Regional Order of Geologists of Sicily (ORGS, Reg. No. 2352); Figshare. https://doi.org/10.6084/m9.figshare.34906956

Hancock, P. A., & Vasmatzidis, I. (2003). Effects of heat stress on cognitive performance: The current state of knowledge. *International Journal of Hyperthermia, 19*(3), 355–372. https://doi.org/10.1080/0265673021000054630

Heidenreich, A., & Thieken, A. H. (2024). Individual heat adaptation: Analyzing risk communication, warnings, heat risk perception, and protective behavior in three German cities. *Risk Analysis, 44*(8), 1788–1808. https://doi.org/10.1111/risa.14278

Hellenic Ministry of Health. (2026, July 20). *Prevention of the health impacts of high temperatures and heatwaves* (Circular Prot. No. D1(d)/GP oik. 34122/20-07-2026, ADA: PSXIE465FYO-DY1) [In Greek]. Directorate of Public Hygiene. https://www.moh.gov.gr/articles/ministry/grafeio-typoy/press-releases/14485-oloklhrwmenos-odhgos-prolhpshs-kai-prostasias-apo-ton-kayswna

Hellenic Ministry of Labour and Social Security. (2024, June 3).

Prevention of heat stress of employees (Circular Prot. No. 34666/03-06-2024, ADA: RG1N46NLDG-OO6) [In Greek]. General Secretariat of Labour Relations, Directorate of Health and Safety at Work. https://ypergasias.gov.gr/lipsi-endedeigmenon-metron-gia-tin-prostasia-ton-ergazomenon-apo-ti-thermiki-kataponisi-ypo-synthikes-kafsona/

Hellenic Ministry of Labour and Social Security. (2026, July 21). *Emergency measures to address heat stress of private-sector employees on Wednesday, July 22, 2026* (Circular Prot. No. 20547/21-07-2026) [In Greek]. General Secretariat of Labour Relations, Directorate of Health and Safety at Work. https://www.ypes.gr/wp-content/uploads/2026/07/eggr20547-20260721.pdf

Hellenic National Meteorological Service (HNMS). (1997). *National Data Bank for Hydrological and Meteorological Information (Hydroscope): Elefsina station (Station ID 20072, Timeseries ID 120, Instrument 2007202, 1951–1996)* [Data set]. http://emy.hydroscope.gr/stations/d/20072/

Hellenic Parliament. (2010). *New architecture of local government and decentralized administration, Kallikratis Programme (Law 3852/2010, Government Gazette 87/A/07-06-2010)* [In Greek]. National Printing House. https://www.et.gr/api/DownloadFeksApi/?fek_pdf=20100100087

Hellenic Republic Open Data Portal. (2026). *HNMS meteorological station 112 (Elefsina Airport automated weather station dataset)* [Data set]. https://data.gov.gr/dataset/emy-station-112

Hellenic Statistical Authority. (2021). *2021 population and housing census of Greece*. https://www.statistics.gr/en/2021-census-res-pop-results

Hellenic Telecommunications and Post Commission. (2006). *Public consultation document regarding the National Numbering Plan* [In Greek]. https://web.archive.org/web/20220124172526/https://www.eett.gr/opencms/export/sites/default/EETT/Electronic_Communications/Telecoms/Numbering/Doc_GR.pdf

Hermides, D., Makri, P., Kontakiotis, G., & Antonarakou, A. (2020). Advances in the coastal and submarine groundwater processes: Controls and environmental impact on the Thriassion Plain and Eleusis Gulf (Attica, Greece). *Journal of Marine Science and Engineering, 8*(11), Article 944. https://doi.org/10.3390/jmse8110944

Hubbard, K. G., Lin, X., & Walter-Shea, E. A. (2001). The effectiveness of the ASOS, MMTS, Gill, and CRS air temperature radiation shields. *Journal of Atmospheric and Oceanic Technology, 18*(6), 851–864. https://doi.org/10.1175/1520-0426(2001)018<0851:TEOTAM>2.0.CO;2

Institute of Local Administration. (2010). *Metropolitan Athens: Spatial and administrative organization* [In Greek]. Central Union of Municipalities and Communities of Greece. https://ita.org.gr/wp-content/uploads/2025/11/mhtropolitikh-athina.pdf

Instituto Português do Mar e da Atmosfera (IPMA). (2025). *Boletim climatológico mensal: Junho 2025* [Monthly climatological bulletin: June 2025; In Portuguese]. https://www.ipma.pt/resources.www/docs/im.publicacoes/edicoes.online/20250721/bSdLZAZThHLdMJajLbQZ/cli_20250601_20250630_pcl_mm_co_pt.pdf

Kallos, G., Kassomenos, P., & Pielke, R. A. (1993). Synoptic and mesoscale weather conditions during air pollution episodes in Athens, Greece. *Boundary-Layer Meteorology, 62*(1–4), 163–184. https://doi.org/10.1007/BF00705553

Karatarakis, N. (2017). *Summer 2017: First heatwave episode 29/6–3/7/2017* [In Greek]. Hellenic National Meteorological Service, Directorate C (Climatology and Applications). https://web.archive.org/web/20171219161939/http://www.hnms.gr/emy/el/pdf/heat_summer_2017.pdf

Kassomenos, P., Kotroni, V., & Kallos, G. (1995). Analysis of climatological and air quality observations from Greater Athens Area. *Atmospheric Environment, 29*(24), 3671–3688. https://doi.org/10.1016/1352-2310(94)00358-R

Kassomenos, P. A., Sindosi, O. A., Lolis, C. J., & Chaloulakou, A. (2003). On the relation between seasonal synoptic circulation types and spatial air quality characteristics in Athens, Greece. *Journal of the Air & Waste Management Association, 53*(3), 309–324. https://doi.org/10.1080/10473289.2003.10466154

Kathimerini. (1977, July 12). Heatwave 1977: Record temperatures across Greece [In Greek]. *Kathimerini*, p. 1.

Koletsis, I., Lagouvardos, K., Kotroni, V., & Proedrou, M. (2009). Numerical study of a katabatic wind event in Athens, Greece. *Natural Hazards and Earth System Sciences, 9*(2), 421–431. https://doi.org/10.5194/nhess-9-421-2009

Kolydas, T. (2023, July 11). *On this day 46 years ago 48 °C were recorded in Elefsina: Historical archive note of the Director of the Hellenic National Meteorological Service (HNMS)* [In Greek]. Thriassio.gr. https://thriassio.gr/san-simera-prin-46-chronia-katagrafikan-48-vathmoi-kelsioy-stin-eleysina/

Lacombe, M., Bousri, D., Leroy, M., & Mezred, M. (2011). *WMO field intercomparison of thermometer screens/shields and humidity measuring instruments: Ghardaïa, Algeria, November 2008–October 2009* (IOM Report No. 106, WMO/TD-No. 1579). World Meteorological Organization. https://web.archive.org/web/20170713123138/https://www.wmo.int/pages/prog/www/IMOP/publications/IOM-106_Ghardaia/IOM-106_Report.pdf

Lagouvardos, K., Kotroni, V., Bezes, A., Koletsis, I., Kopania, T., Lykoudis, S., Mazarakis, N., Papagiannaki, K., & Vougioukas, S. (2017). The automatic weather stations NOANN network of the National Observatory of Athens: Operation and database. *Geoscience Data Journal, 4*(1), 4–16. https://doi.org/10.1002/gdj3.44

Liu, J., Varghese, B. M., Hansen, A., Xiang, J., Zhang, Y., Dear, K., Gourley, M., Driscoll, T., Morgan, G., Capon, A., & Bi, P. (2021). Is there an association between hot weather and poor mental health outcomes? A systematic review and meta-analysis. *Environment International, 153*, Article 106533. https://doi.org/10.1016/j.envint.2021.106533

Lõhmus, M. (2018). Possible biological mechanisms linking mental health and heat—A contemplative review. *International Journal of Environmental Research and Public Health, 15*(7), Article 1515. https://doi.org/10.3390/ijerph15071515

Macedonia. (1977a, July 12). Greece turned into Sahara on Sunday [In Greek]. *Macedonia*, p. 1. http://efimeris.nlg.gr/ns/pdfwin_ftr.asp?c=124&pageid=-1&id=120831&s=0&STEMTYPE=0&STEM_WORD_PHONETIC_IDS=&CropPDF=0

Macedonia. (1977b, July 12). Greece turned into Sahara on Sunday: Detailed meteorological reports [In Greek]. *Macedonia*, p. 3. http://efimeris.nlg.gr/ns/pdfwin_ftr.asp?c=124&pageid=-1&id=120833&s=0&STEMTYPE=0&STEM_WORD_PHONETIC_IDS=&CropPDF=0

Mavrakis, A., Lykoudis, S., Christides, A., Dasaklis, S., Tasopoulos, A., Theoharatos, G., Kyvelou, S., & Verouti, E. (2008). Air quality levels in a closed industrialized basin (Thriassion Plain, Greece). *Fresenius Environmental Bulletin, 17*(4), 443–454.

Mavrakis, A., & Papavasileiou, H. (2013). Relative humidity and land use changes in an environmentally stressed area (Thriasio Plain—Greece). *Procedia Technology, 8*, 471–476. https://doi.org/10.1016/j.protcy.2013.11.061

Mavrakis, A., Spanou, A., Pantavou, K., Katavoutas, G., Theoharatos, G., Christides, A., & Verouti, E. (2012). Biometeorological and air quality assessment in an industrialized area of eastern Mediterranean: The Thriassion Plain, Greece. *International Journal of Biometeorology, 56*(4), 737–747. https://doi.org/10.1007/s00484-011-0475-9

Melas, D., Ziomas, I., Klemm, O., & Zerefos, C. S. (1998). Anatomy of the sea-breeze circulation in Athens area under weak large-scale ambient winds. *Atmospheric Environment, 32*(12), 2223–2237. https://doi.org/10.1016/S1352-2310(97)00420-2

Merlone, A., Pasotti, L., Musacchio, C., Bessemoulin, P., Brunet, M., El Fadli, K., Jones, P., van der Schrier, G., Raspanti, A., Trewin, B., Krahenbuhl, D., & Cerveny, R. (2024). Evaluation of the highest temperature WMO Region VI Europe (continental): 48.8°C, Siracusa Sicilia, Italy on August 11, 2021. *International Journal of Climatology, 44*(3), 721–728. https://doi.org/10.1002/joc.8361

Metaxas, D. A., & Kallos, G. (1980). Heat waves from a synoptic point of view. *Rivista di Meteorologia Aeronautica, 40*(2–3), 107–119.

Meteoclub. (2013). *Historical overview of the HNMS meteorological stations in Nea Filadelfeia* [In Greek]. https://web.archive.org/web/20130706034256/http://www.meteoclub.gr/themata/news/3142-istoriko-stathmoi-emy-neafiladelfia

Météo-France. (2020). *Bilan climatique de l'année 2019 sur la France métropolitaine* [Climatic summary of the year 2019 in metropolitan France; In French]. https://meteofrance.fr/sites/meteofrance.fr/files/files/editorial/Bilan-climatique-annee2019.pdf

Meteology.gr. (2022). *Record of highest temperatures in Europe and other news* [In Greek]. https://web.archive.org/web/20241222080448/https://www.meteology.gr/rekor-ypsiloteron-thermokrasion-eyropis-kai-alla-nea/

MeteoWeb. (2025, July 24). *Caldo in Sicilia, il record europeo di Floridia (Siracusa) dell'agosto 2021 è un clamoroso falso storico* [Heat in Sicily, the European record of Floridia (Syracuse) of August 2021 is a sensational historical falsehood]. https://www.meteoweb.eu/2025/07/caldo-sicilia-record-europeo-floridia-siracusa-agosto-2021-e-clamoroso-falso-storico/1001819097/

Nakamura, R., & Mahrt, L. (2005). Air temperature measurement errors in naturally ventilated radiation shields. *Journal of Atmospheric and Oceanic Technology, 22*(7), 1046–1058. https://doi.org/10.1175/JTECH1762.1

National Observatory of Athens (NOA). (2026). *MeteoSearch climatological data archive* [Data set]. https://meteosearch.meteo.gr/data/index.cfm

Obradovich, N., Migliorini, R., Mednick, S. C., & Fowler, J. H. (2017). Nighttime temperature and human sleep loss in a changing climate. *Science Advances, 3*(5), Article e1601555. https://doi.org/10.1126/sciadv.1601555

Oke, T. R. (1987). *Boundary layer climates* (2nd ed.). Routledge. https://doi.org/10.4324/9780203407219

Oke, T. R., Mills, G., Christen, A., & Voogt, J. A. (2017). *Urban climates*. Cambridge University Press. https://doi.org/10.1017/9781139016476

OpenHI. (2026a). *Hydrometeorological station data: Gyra Stefanis (North Magoula) (2018–2026)* [Data set]. National Observatory of Athens, IAASARS BEYOND; Open Hydrometeorological Information System. https://system.openhi.net/stations/1481/timeseriesgroups/1221/

OpenHI. (2026b). *Hydrometeorological station data: Mandra Stream (Rema) (2020–2026)* [Data set]. National Observatory of Athens, IAASARS BEYOND; Open Hydrometeorological Information System. https://system.openhi.net/stations/8424/

OpenHI. (2026c). *Hydrometeorological station data: Mandra Diversion (Ektropi) (2020–2026)* [Data set]. National Observatory of Athens, IAASARS BEYOND; Open Hydrometeorological Information System. https://system.openhi.net/stations/8425/

OpenHI. (2026d). *Hydrometeorological station data: Mandra Interchange (Komvos) (2020–2026)* [Data set]. National Observatory of Athens, IAASARS BEYOND; Open Hydrometeorological Information System. https://system.openhi.net/stations/8426/timeseriesgroups/888/

Potter, B. E. (2012). Atmospheric interactions with wildland fire behaviour: I. Basic surface interactions, vertical profiles and synoptic structures. *International Journal of Wildland Fire, 21*(7), 779–801. https://doi.org/10.1071/WF11128

Prezerakos, N. G. (1989). A contribution to the study of the extreme heatwave over the South Balkans in July 1987. *Meteorology and Atmospheric Physics, 41*(4), 261–271. https://doi.org/10.1007/BF01026114

Raso, B. (2026, July 24). *Temperature record e propaganda climatica: Il caso del primato di* $+48{,}8^{\circ}$C *in Sicilia finisce al TAR* [Record temperatures and climate propaganda: The case of the $+48.8^{\circ}$C record in Sicily ends up at the Regional Administrative Court]. MeteoWeb. https://www.meteoweb.eu/2026/07/temperature-record-e-propaganda-climatica-il-caso-del-primato-di-488c-in-sicilia-finisce-al-tar/1001960362/

Rizospastis. (1977, July 12). Yesterday's temperatures across Greece [In Greek]. *Rizospastis*, p. 9. http://efimeris.nlg.gr/ns/pdfwin_ftr.asp?c=65&pageid=-1&id=45719&s=0&STEMTYPE=0&STEM_WORD_PHONETIC_IDS=&CropPDF=0

Sailor, D. J. (2011). A review of methods for estimating anthropogenic heat and moisture emissions in the urban environment. *International Journal of Climatology, 31*(2), 189–199. https://doi.org/10.1002/joc.2106

Salvati, L. (2014). The spatial pattern of soil sealing along the urban-rural gradient in a Mediterranean region. *Journal of Environmental Planning and Management, 57*(6), 848–861. https://doi.org/10.1080/09640568.2013.770730

Stull, R. B. (1988). *An introduction to boundary layer meteorology*. Springer. https://doi.org/10.1007/978-94-009-3027-8

Theodor Friedrichs & Co. (1999). *Combined temperature/humidity sensor in shelter Type 3030* (Electrically ventilated versions 3030.1000 and 3030.1100; Technical Datasheet Issue 05.99). Theodor Friedrichs & Co. Meteorologische Geräte und Systeme GmbH.

Theoharatos, G., Pantavou, K., Mavrakis, A., Spanou, A., Katavoutas, G., Efstathiou, P., Mpekas, P., & Asimakopoulos, D. (2010). Heat waves observed in 2007 in Athens, Greece: Synoptic conditions, bioclimatological assessment, air quality levels and health effects. *Environmental Research, 110*(2), 152–161. https://doi.org/10.1016/j.envres.2009.12.002

Tombrou, M., Dandou, A., Helmis, C., Akylas, E., Angelopoulos, G., Flocas, H., Assimakopoulos, V., & Soulakellis, N. (2007). Model evaluation of the atmospheric boundary layer and mixed-layer evolution. *Boundary-Layer Meteorology, 124*(1), 61–79.

https://doi.org/10.1007/s10546-006-9146-5

Tselepidaki, I., Asimakopoulos, D. N., Katsouyanni, K., Moustris, C., Touloumi, G., & Pantazopoulou, A. (1995). The use of a complex thermohygrometric index in predicting adverse health effects in Athens. *International Journal of Biometeorology, 38*(4), 194–198. https://doi.org/10.1007/BF01245388

WeatherLink. (2026). *Aspropyrgos Paralia telemetric weather station bulletin and 10-minute archive* [Data set]. Davis Instruments. https://www.weatherlink.com/bulletin/dcb78353-cde7-4b72-b4de-eaff4d0d67ba

Whiteman, C. D. (2000). *Mountain meteorology: Fundamentals and applications*. Oxford University Press. https://doi.org/10.1093/oso/9780195132717.001.0001

World Meteorological Organization (WMO). (2018). *Guide to instruments and methods of observation* (WMO-No. 8). https://library.wmo.int/idurl/4/41650

World Meteorological Organization (WMO). (2023). *WMO Global Weather and Climate Extremes Archive: Europe: Highest temperature (*48.0°C*, Athens [Elefsina and Tatoi], Greece, 10 July 1977)*. https://web.archive.org/web/20230717201539/https://wmo.asu.edu/content/europe-highest-temperature

World Meteorological Organization (WMO). (2024). *WMO Global Weather and Climate Extremes Archive: Official Region VI (Europe) temperature records*. https://wmo.asu.edu/

World Meteorological Organization (WMO) OSCAR/Surface. (2026a). *Station report details: Aspropyrgos Paralia (WIGOS ID 0-300-1-aspropirgospara)*. https://oscar.wmo.int/surface/#/search/station/stationReportDetails/0-300-1-aspropirgospara

World Meteorological Organization (WMO) OSCAR/Surface. (2026b). *Station report details: Aspropyrgos (WIGOS ID 0-300-1-aspropirgos)*. https://oscar.wmo.int/surface/#/search/station/stationReportDetails/0-300-1-aspropirgos

World Meteorological Organization (WMO) OSCAR/Surface. (2026c). *Station report details: Elefsina (WIGOS ID 0-300-1-elefsina)*. https://oscar.wmo.int/surface/#/search/station/stationReportDetails/0-300-1-elefsina

World Meteorological Organization (WMO) OSCAR/Surface. (2026d). *Station report details: Elefsis Airport (WIGOS ID 0-20000-0-16718)*. https://oscar.wmo.int/surface/#/search/station/stationReportDetails/0-20000-0-16718

Zwiers, F. W., & von Storch, H. (1995). Taking serial correlation into account in tests of the mean. *Journal of Climate, 8*(2), 336–351. https://doi.org/10.1175/1520-0442(1995)008<0336:TSCIAI>2.0.CO;2